



UNIVERSIDADE D
COIMBRA

Inês Tavares da Silva

**DESIGN AND FABRICATION OF SOFT GRASPING
MECHANISMS**

Dissertação no âmbito do Mestrado em Engenharia Mecânica, na área de Produção e Projeto, orientada pelo Professor Doutor Pedro Mariano Simões Neto e apresentada ao Departamento de Engenharia Mecânica da Faculdade de Ciências e Tecnologia da Universidade de Coimbra.

Setembro de 2023

1 2



9 0

FACULDADE DE
CIÊNCIAS E TECNOLOGIA
UNIVERSIDADE DE
COIMBRA

Design and fabrication of soft grasping mechanisms

A dissertation submitted in partial fulfilment of the requirements for the degree of Master in Mechanical Engineering in the speciality of Manufacturing and Design

Projeto e manufatura de mecanismos *soft*

Author

Inês Tavares da Silva

Advisor

Pedro Mariano Simões Neto

Committee

Chair

Professor Doutor José Luís Ferreira Afonso
Professor Auxiliar da Universidade de Coimbra

Member

Professor Doutor Paulo Joaquim Antunes Vaz
Professor Adjunto do Instituto Politécnico de Viseu

Advisor

Professor Doutor Pedro Mariano Simões Neto
Professor Auxiliar da Universidade de Coimbra

Coimbra, September, 2023

The future is almost here. And it is squishy.

[James MacDonald, in JSTOR Daily, 2016.]

Aos meus pais.

ACKNOWLEDGEMENTS

I would like to express my heartfelt gratitude to all the individuals who contributed to this dissertation. I am deeply thankful for the support I received throughout my five years at university.

I am especially grateful for my parents and all they have done to see me happy. Their motivation and encouragement have been invaluable, and without them, this work would not have been possible. Thank you for all the support and for encouraging me to follow my dreams.

To my advisor, Professor Dr. Pedro Neto, for trusting me with the opportunity to develop this project at CoRLUC, and for his guidance throughout this journey. His availability and mentorship have been crucial to my academic growth.

I would like to acknowledge Professor Dr. José Afonso for his help and assistance at various stages of my academic journey. His patience and guidance have been greatly appreciated.

My gratitude also goes out to my colleagues (now friends) from the laboratory. Thank you for all the insights, guidance, encouragement, and for helping me overcome the challenges of this research.

Speaking of friends, I am grateful for the friendships I have cultivated throughout my university years and for the friends I already had from high school. They have provided me with cherished memories and much-needed mental rest.

Last, but certainly not least, I want to express my deepest gratitude to my boyfriend, Hugo, for his unwavering support and affection. His encouragement and motivation have been the pillars of strength on which I leaned during the less inspiring days of this academic journey. Thank you for everything.

Abstract

Soft robotics, characterized by flexible and deformable structures, has emerged as a promising field to address some limitations in traditional rigid robotics. While rigid robots excel in precision and strength, they often lack the adaptability and safety required for human interaction and delicate tasks.

This dissertation explores ways to improve an already existing flexible and pneumatically actuated robotic hand, such as the optimization of fabrication processes and enhancing the hand's functionality.

Several changes have been incorporated to the robotic hand, such as the adoption of more flexible materials, adjustments to the hand's geometry and thickness, the integration of silicone to the palm to amplify the coefficient of friction, and the implementation of a new actuator reinforcement method, using a unidirectional elastic bandage as reinforcement.

These adaptations have undergone testing and have demonstrated several notable improvements. One such test involved a cyclic loading examination, where the force required to bend a variety of sample fingers to a specific angle was measured, along with the angle at which these fingers naturally returned when not subjected to flexion. Some tests were conducted on the actuators in relation to the pressure applied, such as horizontal displacement, bending angles, and finger force.

The actuators are now more resistant to tearing and more stretchable, which allows the fingers to apply greater force during closure and achieve more extensive closing angles. The modified geometry enhances object grasping as the hand conforms more effectively around objects. Additionally, the bending resistance in the fingers has decreased, requiring less pressure to achieve the same bending angles.

Keywords: Soft robotics, Soft materials, Reinforced actuator, Pneumatic robotic hand, Unidirectional elastic bandage.

Resumo

A robótica *soft*, caracterizada por estruturas flexíveis e deformáveis, surge como uma área promissora para superar algumas limitações da robótica rígida tradicional. Embora os robôs rígidos se destaquem pela sua precisão e força, frequentemente carecem da adaptabilidade e segurança necessárias para interação com seres humanos e tarefas delicadas.

Esta dissertação explora maneiras de melhorar uma mão robótica flexível e atuada pneumaticamente já existente, como a otimização de processos de fabrico e o aprimorar da funcionalidade da mão.

Várias alterações foram feitas na mão robótica, como a adoção de materiais mais flexíveis, ajustes na geometria e espessura da mão, a integração de silicone na palma da mão para aumentar o coeficiente de atrito e a implementação de um novo método de reforço do atuador, usando uma ligadura unidirecionalmente elástica.

Estas adaptações foram submetidas a uma série de testes que revelaram diversas melhorias notáveis. Um desses testes envolveu uma análise de carga cíclica, na qual a quantidade de força necessária para dobrar uma variedade de dedos de amostra até um ângulo específico foi medida, bem como o ângulo ao qual os dedos naturalmente retornavam quando não estavam sob flexão. Além disso, outros testes foram realizados nos atuadores em relação à pressão aplicada nos mesmos, incluindo avaliações da deformação, ângulos de flexão e a força exercida pelos dedos.

Os atuadores são, agora, mais resistentes a rasgos e mais elásticos, o que permite que os dedos exerçam maior força durante a sua flexão e alcancem ângulos de curvatura mais amplos. As alterações à geometria melhoram a capacidade de agarrar objetos, uma vez que a mão se adapta mais eficazmente em torno deles. Para além disso, a resistência à flexão dos dedos diminuiu, exigindo menos pressão exercida nos atuadores para alcançar os mesmos ângulos de flexão.

Palavras-chave: Robótica *soft*, Materiais suaves, Atuador reforçado, Mão robótica pneumática, Ligadura unidirecionalmente elástica.

Contents

LIST OF FIGURES	ix
LIST OF TABLES.....	xi
LIST OF ACRONYMS/ ABBREVIATIONS.....	xiii
1. Introduction	1
2. State of the art.....	3
2.1. Soft Robotics.....	3
2.1.1. Soft Grippers.....	4
2.2. Fatigue/Cyclical Test.....	10
3. Proposed Approach.....	13
3.1. Basic Functioning of the Robotic Hand.....	13
3.2. Facilitating Finger Bending	14
3.3. Fabrication Process of the Actuators	17
3.4. Enhancing Hand Grip.....	23
3.4.1. Exoskeleton's Geometry.....	23
3.4.2. Improving Coefficient of Friction	24
4. Experiments and Results	25
4.1. Fatigue/Cyclical Tests.....	25
4.1.1. Materials	25
4.1.2. Geometry	27
4.1.3. Thickness.....	29
4.2. Pressure Related Tests	29
4.2.1. Horizontal Displacement	30
4.2.2. Folding Angle.....	32
4.2.3. Finger Force.....	34
5. Conclusions	37
5.1. Future Work.....	39
REFERENCES	41

LIST OF FIGURES

Figure 2.1. Examples of different finger arrangements: (a) with axial and (b) linear symmetry, (c) human-inspired hand [4].	5
Figure 2.2. Mushroom-shaped geometry patterns [7].	6
Figure 2.3. The hierarchical fibrillar structure of a gecko's toe. (a) A gecko clinging to a surface with only one finger [15]; (b) Gecko toe pads [17]; (c) Lamellae [17]; (d) Top view of setal arrays [17]; (e) Side view of setal arrays [17]; (f) Spatulae [17]; (g) Spatula (SP) [18].	7
Figure 2.4. (a) Gecko toe pads flat on a glass surface; (b) Gecko toe pads hyperextended to release the surface so they can move [15].	8
Figure 2.5. (a) schematic view of the designed multilegged LCN-based gripper; (b) gripping facilitated by an electromagnet and (c) releasing induced by thermal deformation of hybrid LCN cantilevers [12].	8
Figure 2.6. Actuation of magnetic micropillars under the microscope. (a) Top and side view of the actuation where in the presence of a magnetic field, the micropillars completely flatten [20]. (b)-(d) Tilting, observed in the magnetic micropillars, to opposite directions when the magnet is approached from opposite sides [21]. (e)-(f) Tilting observed in the magnetic micropillars at stronger field gradients [21].	9
Figure 3.1. (a) Different layers of the reinforced actuators; (b) Geometry of the exoskeleton's finger.	13
Figure 3.2. Representation of the elastic (in green) and non-elastic (in red) fibres of the <i>Hansaplast</i> unidirectional elastic fixation bandage.	14
Figure 3.3. (a) Mechanism assembled for the cyclic loading test; (b) Representation of the load cell used; (c) Representation of the load cell amplifier used; (d) Depiction of the servo motor used.	16
Figure 3.4. Original joint geometry (left) and new joint geometry/crease (right).	16
Figure 3.5. The four steps used in the construction of the actuators for the first version of the hand [1].	18
Figure 3.6. Unidirectional elastic bandage revolved around the core of the mould.	19
Figure 3.7. Before (left) and after (right) the modifications made to the sealing component for the actuator's base.	21
Figure 3.8. Some modifications made to the exoskeleton.	24
Figure 3.9. (a) Incorporation of silicone strips into the palm of the robotic hand; (b) Successful gripping and retention of objects by the robotic hand, showcasing the practical benefits of the silicone strip integration.	24
Figure 4.1. (a) Compilation of the results for maximum force applied (per cycle) to each sample finger printed in (b) Filaflex 70A, (c) Ninjaflex and (d) Smartfil Flex 93A.	26

Figure 4.2. Angle (per cycle) at which the load cell touches each sample finger, all printed in different materials.	27
Figure 4.3. Maximum force applied (per cycle) to sample fingers with and without a triangular groove in the joint areas.....	27
Figure 4.4. Compilation of all the results for the angles (per cycle) at which the load cell touches the sample finger with a triangular groove.	28
Figure 4.5. Maximum force applied to sample fingers with different thicknesses and angles at which the load cell touches the finger.....	29
Figure 4.6. Horizontal displacement results compared between the new reinforcement method (on the left) and the initial one (on the right) [1], both fabricated with <i>Ecoflex 00-50</i>	31
Figure 4.7. Horizontal displacement results for the actuator fabricated with the new reinforcement method using <i>Ecoflex 00-30</i>	31
Figure 4.8. True displacement values corrected for the actuator curvature.	32
Figure 4.9. Horizontal displacement in relation to the pressure applied to the actuator for different silicones, <i>Ecoflex 00-50</i> and <i>Ecoflex 00-30</i> (accounting for curvature correction), and reinforcements, PET thread and unidirectional elastic fabric for reinforcements.....	32
Figure 4.10. Results of the folding angles at 0 kPa (at the top) and at 60 kPa (at the bottom) using the new actuators with unidirectional elastic fabric reinforcement, one with <i>Ecoflex 00-30</i> (at the left) and the other with <i>Ecoflex 00-50</i> (at the right), and the initial version of the actuator (in the centre) [1].....	33
Figure 4.11. Folding angles in relation to the pressure being applied (from 0 kPa to 60 kPa).	34
Figure 4.12. Finger force applied to the weighting scale in relation to the pressure (from 0 kPa to 80 kPa).	35

LIST OF TABLES

Table 3.1. Technical overview of two silicone types. 22
Table 4.1 Technical overview of three TPU materials. 25

LIST OF ACRONYMS/ ABBREVIATIONS

- 3D – Three dimensions
- CAD – Computer-aided design
- FDM – Fused deposition modelling
- FFF – Fused filament fabrication
- LCN – Liquid crystalline network
- PET – Polyethylene terephthalate
- PLA – Polylactic acid
- TPU – Thermoplastic polyurethane

1. INTRODUCTION

For many years, humans have relied on robots to handle tasks demanding high precision, speed, strength, and accessing remote or dangerous locations beyond human reach. While conventional rigid robots have served extensively in industrial and research settings, their strength and speed can also make them unsafe. As such, some rigid robots have considerably limited interaction with their surroundings, particularly with people. Furthermore, rigid robots are also not well-suited for handling fragile objects due to their inability to deform around them. Consequently, the need to explore alternatives that are more flexible, malleable, and elastic emerged, leading to the phenomenon of soft robotics.

A soft robot is a flexible mechanism with a compliant body, made with materials such as elastomers capable of significant deformations. The adoption of 3D printers to fabricate flexible objects and rigid moulds for manufacturing silicone pneumatic actuators has marked a significant breakthrough in the realm of soft robotics.

One example of such silicone pneumatic actuator has been manufactured for use in a flexible and pneumatically actuated robotic hand [1]. While this work was pioneering and made valuable contributions, certain areas have been identified for potential improvement to enhance the efficacy and functionality of the soft hand. Some of the challenges in functionality include insufficient force of the pneumatic actuators, an inefficient hand geometry, a time-consuming and intricate actuator manufacturing process, frequent air leaks due to actuator ruptures under high pressures, and unsatisfactory object grasping with tendency to slip during handling.

Based on these observations, there is a need to improve the original design. The proposed changes aim to optimize the fabrication process and enhance the functionality of the hand, providing a greater range of finger movements as well as a more precise grip when handling objects.

Therefore, some of the changes implemented include adjusting the hand's geometry, using a different material for printing the exoskeleton, adopting a new manufacturing process for the actuators that includes a different type of reinforcement, and integrating silicone strips on the palms for improved coefficient of friction and consequent object grasping.

It is important to emphasize that these improvements do not diminish the previous work done on this topic, on the contrary, they build upon the previous achievements and aim to further expand the field of soft robotics.

This dissertation is structured into five chapters. Chapter one introduces the theme, discusses the problem, motivation and outlines the proposed approach. In the second chapter, a literature review is conducted on key topics relevant to this study. Chapter three provides an in-depth explanation of hand functionality, offers a detailed problem description, and explores the approaches used to address it. Chapter four focuses on the analysis of the experiment results. Finally, the concluding chapter draws some conclusions from these results and presents suggestions for future research within this field.

2. STATE OF THE ART

Surprisingly enough, the phenomenon of robotics has its roots in a time predating the discovery of electricity itself, long before the arrival of modern robotics as we know it today. Interestingly, the term “robot” emerged relatively recently, about a century ago, with an intriguing origin in the Czech word “*robota*” meaning “servitude” or “forced labour”.

While the term "robot" often brings to mind images of metallic, futuristic humanoids, this association is not always accurate. In reality, a robot is simply a machine designed to accomplish a task with minimal to no human interaction. The robots we encounter in present times are frequently employed to replace human labour. Yet, they have evolved from their ancestors, with origins that extend far before the existence of the term "robot". For instance, over 4000 years ago, Egypt witnessed the creation of automatons capable of basic movements and even generating sounds. These early automatons primarily served as sources of entertainment, in contrast to the modern robots that fulfil a wide range of intricate tasks. Nevertheless, it is essential to recognize these historical machines as the early examples to the robots we encounter today.

2.1. Soft Robotics

Although the effort to create robots that differ from the conventional rigid ones has existed for over half a century, the term "soft robotics" was only created in the early 2000s. In recent years, soft robotics has emerged as one of the fastest-growing categories in the field, gaining great popularity in the robotics community during the last decade.

The key advantage of soft robots lies precisely in their softness and flexibility, making them a safer option in many scenarios. Unlike rigid robots, they do not demand pinpoint precision in their movements, as their soft nature absorbs impacts and enhances their adaptability, reducing potential damage resulted from slight deviations in intended actions. Additionally, the malleability of soft robots allows for shaping them into various forms, such as those produced with silicone using cast moulding technology in PLA moulds. This flexibility enables the creation of robots in virtually any desired shape, even mimicking some shapes found in nature, drawing inspiration from living beings and harnessing the work of nature, an essential influence on the development of soft robotics.

Traditional soft robots are known for their flexibility but often encounter difficulties when navigating cluttered environments with varying curvatures. To address this challenge, a recent study took inspiration from the manoeuvrability exhibited by an elephant's trunk [2]. In this research, a soft robot using soft pneumatic actuators and interference plates was developed. These plates enable the robot to adjust its stiffness in specific areas, like having different levels of flexibility in different parts of the trunk. This innovative approach could lead to more advanced soft robots that combine insights from nature's design.

A specific subset of soft robotics involves soft pneumatic actuators, which traditionally use single materials like silicone, fabrics, or thermoplastic polyurethane (TPU), each with its limitations. However, a new study explores a new composite actuator design that combines silicone polymers and 3D-printed TPU using fused deposition modelling (FDM) [3]. Silicone's high strain capacity acts as an inner seal, while 3D-printed TPU serves as an external constraint, controlling deformation. This composite design produces actuators that endure higher stress, create significant deformations at lower pressures, and even offer reconfigurability by modifying the inner silicone bladder and external skin to adjust actuator properties.

2.1.1. Soft Grippers

When discussing gripping devices, it is important to distinguish between active and passive gripping. Active grippers require constant actuation throughout the entire gripping process to sustain the gripping force, resulting in continuous pressurization. Passive grippers, on the other hand, do not require constant actuation to maintain their gripping force.

Currently, most soft grippers use active gripping principles to grip onto other objects. Although this type of actuation is the most common, it has some disadvantages. Active grippers are often powered by external sources such as motors or pressurized air. However, continuous pressurization can lead to accidents caused by high strain deformations of the soft materials and material wear off. Additionally, active grippers are often limited as their design requires the objects to fit within a predefined region enclosed by the gripper's links. This can make them less versatile and less suitable for tasks that involve gripping objects of different sizes and shapes.

Passive grippers, on the other hand, can be more energy-efficient and require less maintenance, making them ideal for applications where a constant power source may not be

available or practical. These grippers rely on materials with unique adhesive properties, such as gecko-inspired adhesives, to achieve and maintain their gripping force without the need for external power sources.

2.1.1.1. Active Grippers

In the domain of soft grippers, a design concept emerges for a flexible gripper dedicated to delicately handle objects. Constructed exclusively from flexible materials like rubber and silicone, this gripper conforms to complex object shapes and demonstrates adaptability through the deformation of its body using soft pneumatic actuators developed by the authors [4]. Its configuration can be easily adjusted, which demonstrates versatility, enabling customization for specific tasks. Some of this gripper's configurations include finger arrangements with axial and linear symmetry, as for a human-inspired hand (as depicted in Figure 2.1). This study provides valuable insights into the designs and experimental characterization in soft grippers, enhancing the field's understanding of adaptable solutions for delicate object manipulation.

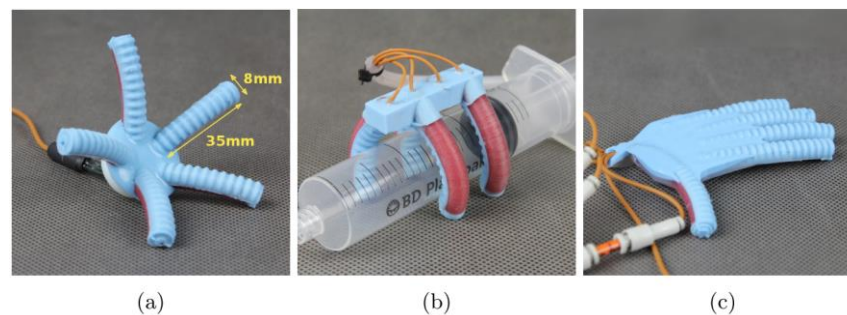


Figure 2.1. Examples of different finger arrangements: (a) with axial and (b) linear symmetry, (c) human-inspired hand [4].

The human hand is remarkable for its ability to handle objects of different shapes, weights, and textures with strength and precision. However, modern prosthetic devices that aim to replicate these functions often become too complex and expensive, with many precise parts like small motors and sensors, along with complicated control systems. To surpass this problem, Fras J. and Althoefer K. introduce a soft pneumatic hand as a simpler and more affordable solution [5]. This hand comprises a total of six actuators with fibre reinforcement. An exoskeleton structure is strategically used to constrain the actuators' deformations in certain areas, transforming the linear deformation of the actuator in finger bending movement. Each finger is individually powered by one actuator, while the thumb has two actuators, enabling both opposition and repositioning movements. This hand can adapt to

the objects it handles without needing complex controls, using only air pressure. It allows for individual finger control and can be customized to fit each user's needs.

2.1.1.2. Passive Grippers

Recent advancements in soft robotics' research have emphasized the necessity of developing robotic grippers capable of securely grasping objects of various geometries and sizes. One approach to accomplishing this includes gripper materials that exhibit higher friction coefficients. Among the possible materials that satisfy this requirement, silicone-based materials have emerged as a leading candidate due to their excellent gripping properties. For that reason, silicone elastomers are frequently used for most soft grippers.

Silicone is valued not only for its high friction coefficient but also for its flexibility and ability to take on a variety of shapes through moulding. This versatility is particularly advantageous because, aside from the material's friction coefficient, modifying the surface itself by adding micro- and nanometric structures is another method to increase adhesion. Various adhesive structure geometries have been studied, such as spherical, flat or nanoscale hair-like structures. However, the mushroom-shaped geometries, which provide a higher adhesive force and are represented in Figure 2.2, have been shown to be the most effective [6]. Due to their superior adhesive properties, several studies have been conducted to develop and use these geometry patterns on grippers' surfaces for higher adhesion.

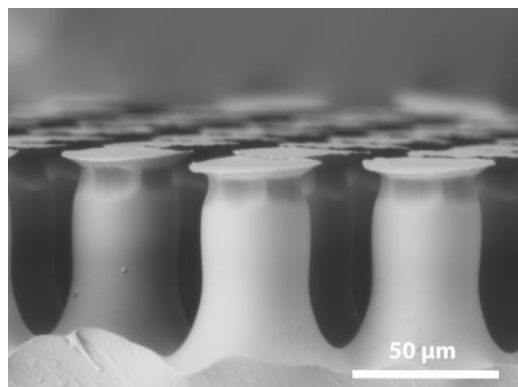


Figure 2.2. Mushroom-shaped geometry patterns [7].

In contrast to most man-made devices, geckos have the remarkable ability to walk on vertical and inverted surfaces without the aid of vacuum suction, magnets, Velcro, chemical adhesion, or electromagnetic interactions. Instead, geckos use the nanometric lamellar setae structures located on their feet and tail to attach to surfaces. As shown in Figure 2.3, their toes consist of hundreds of thousands of fibrillar structures called setae and each one splits

into hundreds of spatulae [8], [9]. These structures interact with the surface on the atomic level, creating van der Waals forces between the atoms of the setae and the atoms of the surface, which are strong enough to hold the gecko in place [9]–[16]. What's even more impressive is that geckos can attach to surfaces in all kinds of conditions, including wet, dry, rough, smooth, clean, and dirty surfaces [8]. While the force produced by a single spatula is relatively weak, considering that van der Waals forces are the weakest intermolecular forces, the collective effect of approximately 2 million spatulae on a gecko's toe becomes strong enough to enable the gecko to adhere to surfaces using just a single toe [15], as shown in Figure 2.3 (a).

This behaviour has inspired the development of gecko-inspired adhesives, also known as “Gecko Tape” or “Nano Tape”, that exhibit similar properties and work effectively under a wide range of conditions. By studying gecko adhesion, scientists hope to develop new adhesives and gripping devices that can be used in a variety of applications, from robotics and aerospace engineering to medical devices and sports equipment.

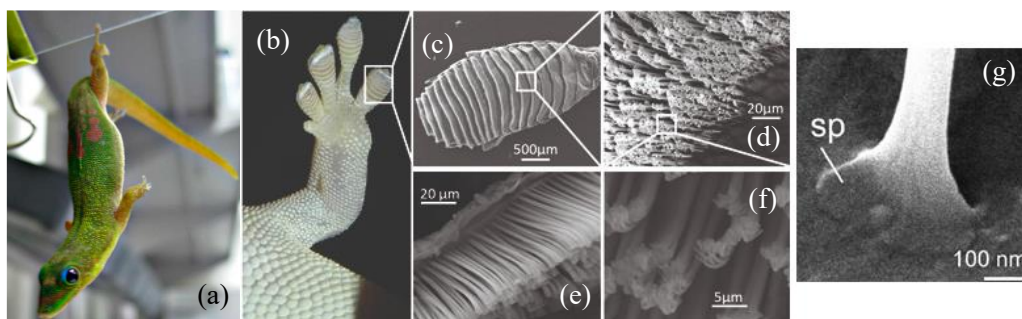


Figure 2.3. The hierarchical fibrillar structure of a gecko's toe. (a) A gecko clinging to a surface with only one finger [15]; (b) Gecko toe pads [17]; (c) Lamellae [17]; (d) Top view of setal arrays [17]; (e) Side view of setal arrays [17]; (f) Spatulae [17]; (g) Spatula (SP) [18].

As previously explained, geckos demonstrate a remarkable ability to adhere to surfaces, enabling them to navigate diverse environments and avoid potential threats. However, since adhesion is proportional to contact area, in order to achieve rapid movements, geckos detach from surfaces by curling/hyperextending the muscles of their toes upward, as illustrated in Figure 2.4, minimizing the contact area and facilitating separation.

Researchers have made strides in developing artificial muscles that emulate geckos' toe muscles/movements and adhesive surface morphologies that resemble geckos' passive adhesive structures.

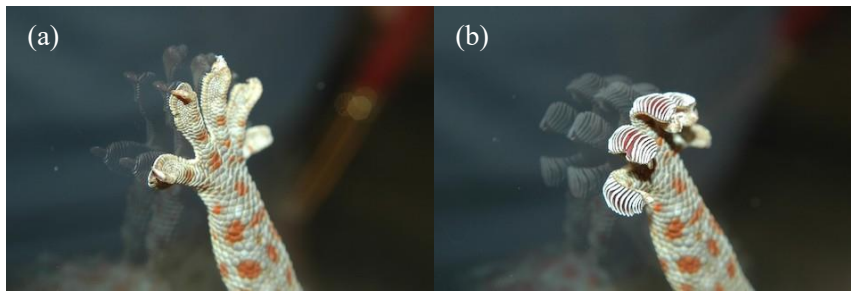


Figure 2.4. (a) Gecko toe pads flat on a glass surface; (b) Gecko toe pads hyperextended to release the surface so they can move [15].

For instance, a recent study introduced a gecko-inspired soft gripper with switchable adhesion controlled by air pressure, where positive pressure resulted in high adhesion and negative pressure in low adhesion [19]. In this study, mushroom-shaped geometry patterns were used as the adhesive structures and the air pressure worked as artificial toe muscles.

Another research project involved a thermally active gripper based on switchable adhesion by mimicking the self-peeling capacity of gecko toe pads, where “releasing was triggered by temperature-driven bending of” liquid crystalline network (LCN) cantilevers “that caused peeling of the adhesive patch”, as Shahsavan et al. stated [12]. On the other hand, gripping was facilitated by magnetic patches attached to the upper side of the cantilevers, as highlighted in Figure 2.5 (b). This feature was incorporated in response to the need for adequate preload stress during the approaching phase.

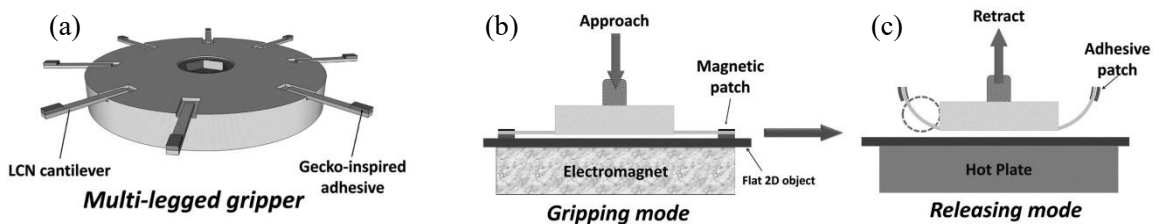


Figure 2.5. (a) schematic view of the designed multilegged LCN-based gripper; (b) gripping facilitated by an electromagnet and (c) releasing induced by thermal deformation of hybrid LCN cantilevers [12].

A question arises regarding how geckos are able to achieve fast running speeds while coordinating these “on-off” toe movements with each step. It has been discovered that their adhesive mechanism is not solely dependent on muscle action. In fact, researchers have further uncovered the significance of the angle of geckos’ setae [10], [12], [15]. During detachment, setal arrays are arranged in a critical angle to facilitate releasing of the toe pads. The oblique angle of the setae allows geckos to maintain partial adhesion to horizontal surfaces while running at high speeds. For that reason, geckos often run with their toes lifted,

which lets them achieve greater running velocity without fully compromising their adhesive abilities [15].

Considering adhesion also depends on the setae angle, researchers have investigated the use of a composite material consisting of an adhesive polymer film and magnetic nickel cantilevers with controllable orientation via a magnetic field [10]. In this particular study, the nickel cantilevers functioned as setal arrays, in contrast to the cantilevers observed in Shahsavan et al.'s research, which served as the gripper's fingers. When subjected to a magnetic field, the nickel beams reorient themselves, causing the terminal pad of the structure, which is responsible for adhesion, to rotate away from the surface. Consequently, the contact area is reduced, causing the adhesion to decrease by a factor of 40. This material has shown promise as a means of decreasing adhesion. Similar methods were used in publications [20] and [21], the last one assuring that this approach allows for control over the adhesive force and detachment process.

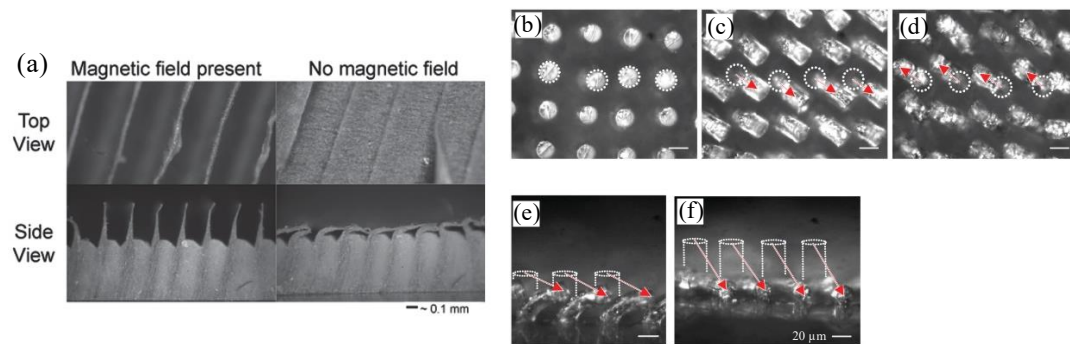


Figure 2.6. Actuation of magnetic micropillars under the microscope. (a) Top and side view of the actuation where in the presence of a magnetic field, the micropillars completely flatten [20]. (b)-(d) Tilting, observed in the magnetic micropillars, to opposite directions when the magnet is approached from opposite sides [21]. (e)-(f) Tilting observed in the magnetic micropillars at stronger field gradients [21].

These studies represent only a small fraction of the extensive research conducted on the utilization of gecko-inspired structures and movements to design soft grippers with enhanced capabilities. Some other approaches include a controllable anisotropic dry adhesive, which is fabricated using ultraprecision diamond cutting [13], and a shape memory polymer surface where the shape of the microstructures can be switched in response to temperature [22].

2.2. Fatigue/Cyclical Test

Material fatigue testing, also known as load cyclic testing, is a mechanical testing method used to assess the behaviour and durability of materials subjected to repeated or cyclic loading. This type of testing is crucial for understanding how materials, such as metals, polymers, composites, and other materials, respond to the stresses and strains they experience in real-world applications, especially those involving repetitive loading. The key components of material fatigue testing include subjecting a sample to a cyclic or alternating load, typically by applying tension and compression forces, while monitoring the sample's response over time. The primary purpose of this testing is to determine how many cycles or repetitions of loading a material can endure before it fails, commonly referred to as the fatigue life. In most applications, an actuator's fatigue life stands as a crucial factor in determining its suitability. Consequently, a longer fatigue life renders an actuator viable for a wider range of applications.

Woods B. et al. discussed fatigue testing for pneumatic artificial muscles, which are commonly used in robotics due to their simplicity and impressive performance [23]. However, they usually wear out quickly, typically lasting less than 18,000 cycles. The main goal of the study was to develop a new method to make these muscles last much longer. By using a process called swaging, stress concentrations were reduced, and mechanical strength was improved. As a result, the muscles could endure over 120 million cycles in realistic operating conditions, a significant improvement from their original lifespan.

Jiang Y. et al. conducted a study on the fatigue behaviour of pneumatic actuators used in rehabilitation exercises for patients with hand pathologies, produced using an innovative fabrication method combining the principles of lost-wax and inverse flow injection [24]. This last method involves injecting degassed liquid silicone from the bottom of the mould to minimize the presence of air bubbles. The results revealed that actuators manufactured using this new technique could endure pressures 2.5 times higher before rupturing, leading to a significant increase in their fatigue life.

Wenlin C. et al. conducted a study on the impact of fatigue on pneumatic artificial muscles [25]. Their findings indicated that, when subjected to a pressure of 2 bar, the actuators could withstand over 20,000 cycles. Furthermore, the primary mode of fatigue failure observed was the development of air leaks in the middle of the actuator.

Zaghloul A. et al. enhanced origami-inspired soft pneumatic actuators with an accordion-like crease pattern, achieved through the utilization of a heat-shrink tube and a reusable mould [26]. Fatigue testing conducted on these actuators demonstrated their capability to withstand 150,000 cycles under a 2 kg load. After testing, the actuators remained in excellent condition, exhibiting no defects such as cracks or holes. This represents a noteworthy advancement, as earlier designs experienced failure at only half the load and with fewer cycles.

Patel D. et al. developed a soft locomotion robot [27]. The actuators consist of a pre-stretched membrane enclosed between two 3D printed frames containing embedded shape memory alloy coils. Applying an electric potential difference to the coils induces bending in the actuator. Cyclic testing was carried out to assess the impact of fatigue on the attained curvature, revealing that after 580 cycles, no changes were detected.

3. PROPOSED APPROACH

3.1. Basic Functioning of the Robotic Hand

The soft robotic hand consists of two fundamental parts: the exoskeleton and the reinforced actuators.

The exoskeleton defines the hand's shape, serving as its outer structure. It is designed in a CAD Software, more specifically *Autodesk Inventor 2023*, and fabricated using the Fused Filament Fabrication (FFF) manufacturing process. Consequently, it is 3D printed in a *Prusa i3 MK3S+* with a TPU filament, the *Filaflex 70A*. This polymeric material is both flexible and elastic, behaving similarly to rubber, as it combines elastomer characteristics with those of thermoplastics.

The actuators are partly made of silicone, which is poured into moulds when still in its liquid state, before undergoing the curing process. This process is often referred to as cast moulding. The moulds are 3D printed using a PLA filament and also designed using *Autodesk Inventor 2023*.

The actuators were reinforced with a unidirectional elastic fixation bandage, more specifically from the brand *Hansaplast*, wrapped between the two silicone layers (refer to Figure 3.1 (a)), to restrict radial expansion and enable only longitudinal deformation. This bandage incorporates non-elastic fibres in one direction, while integrating elastic ones in the perpendicular direction (Figure 3.2).

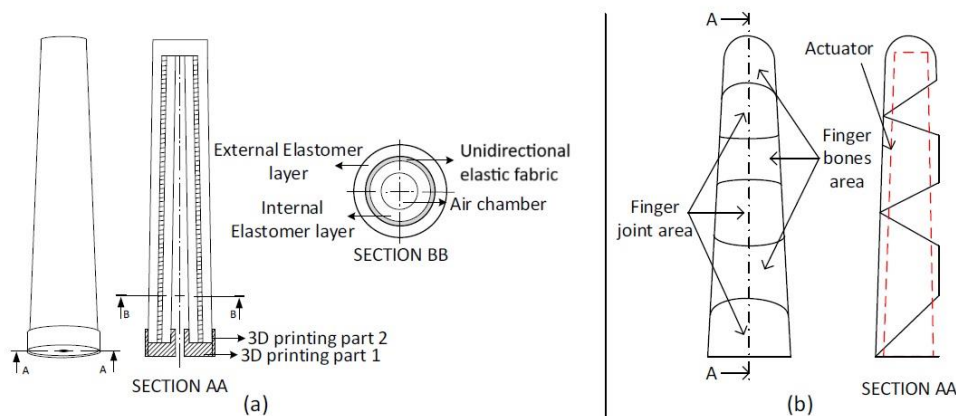


Figure 3.1. (a) Different layers of the reinforced actuators; (b) Geometry of the exoskeleton's finger.

In an unreinforced actuator, upon pressurization, the actuator would expand in every direction, both radial and longitudinal. However, in this context, radial expansion is not necessary and, in fact, undesirable, as bubbles could form in the open areas of the exoskeleton's fingers (Figure 3.1 (b)) and, consequently, burst, resulting in air leaks.

With the elastic bandage reinforcement, upon pressurization, the actuator will only stretch longitudinally, as the non-elastic fibres prevent radial expansion. This only happens when the elastic fibres are oriented longitudinally, and the non-elastic ones are wrapped around the actuator.

Despite the exoskeleton's material being relatively elastic, it is stiffer than the actuators' material, leading to limited stretch while maintaining flexibility. Consequently, when the actuators inflate and extend, given that the exoskeleton's fingertip areas are enclosed, the inflated actuators drive the fingertips in the direction of their extension. However, due to the fingers' walls not being fully closed in the joint areas, the actuators bend the fingers instead of extending them longitudinally. This occurs because, as the actuators extend and reach the fingertips, they encounter no room for further stretching, leading them to expand into the free areas within the joints.



Figure 3.2. Representation of the elastic (in green) and non-elastic (in red) fibres of the *Hansaplast* unidirectional elastic fixation bandage.

3.2. Facilitating Finger Bending

Upon examining the hand that served as inspiration for this dissertation [1], several challenges affecting its functionality were observed.

Firstly, there is a limitation in achieving complete closure of the fingers. One of the contributing factors is the material used to print the exoskeleton. With the availability of new, highly flexible filaments, it's possible to reduce the resistive force in the fingers and,

therefore, the pressure required for finger bending, preventing the actuators from protruding from the exoskeleton by escaping through the holes. This occurrence can also be attributed to the insufficient force exerted by the pneumatic actuators responsible for bending the fingers.

An optimization of printing parameters was conducted, with one of the most crucial factors being filament retraction. This is particularly significant in the printing of flexible materials like TPU, which tend to leave stringing in the absence of this printing option. Consequently, the retraction feature was enabled (3 mm), resulting in an enhancement of print quality.

To facilitate the bending of the finger, three different approaches involving the exoskeleton were tested, which were: Testing three different materials; Changing the geometry of the finger joints; Adjusting the thickness of the fingers' walls.

Each approach was tested through a cyclic loading test using a *DSS-M15S 270°* servo motor and a *CZL635-5kg* load cell (connected to a *HX711* load cell amplifier), both controlled by an Arduino board.

During each cycle, the servo motor would rotate between 120 and 80 degrees and the load cell, connected to the motor, would rotate by association and bend a sample finger, measuring the force applied (depicted in Figure 3.3). The angle at which the load cell contacted the finger was calculated for every cycle, afterwards, using the load data. This angle corresponds to the position to which the finger returns at the end of each cycle.

This cyclic loading test enables the analysis of changes in the maximum applied load per cycle and the evaluation of whether the finger retains its capacity to return to its initial position. If the finger loses its elastic memory, this would be evident through changes in the angle at which the load cell touches the finger.

Five to eight tests were conducted on each sample finger, with the exact number depending on the results obtained. If there were many inconclusive results, additional tests were performed to ensure accuracy.

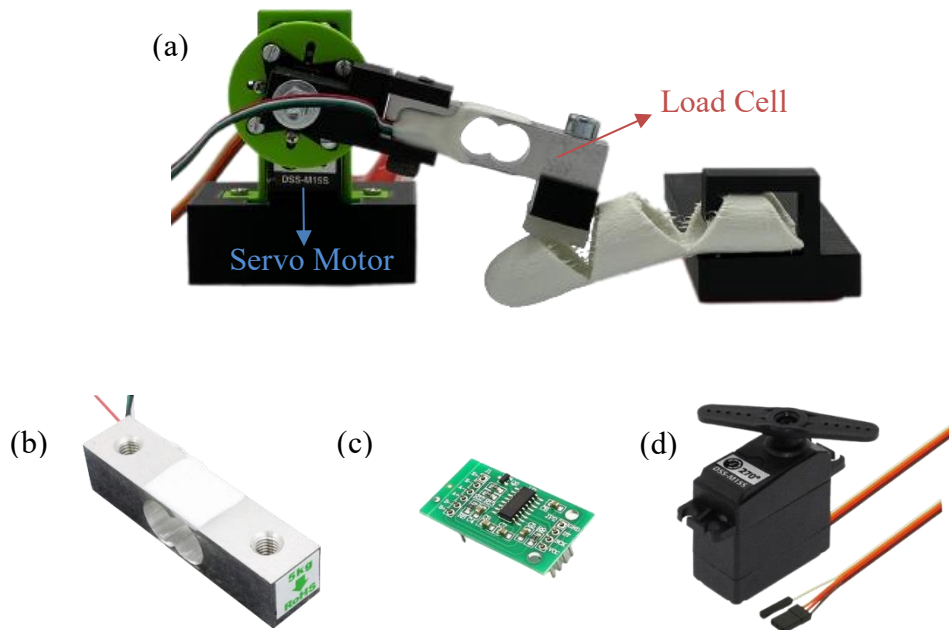


Figure 3.3. (a) Mechanism assembled for the cyclic loading test; (b) Representation of the load cell used; (c) Representation of the load cell amplifier used; (d) Depiction of the servo motor used.

Initially, this test was carried out on three different fingers, each fabricated with a different material while maintaining the same geometry and thickness. The different filaments used to print the three different fingers, listed in decreasing order of hardness, were *Smartfil Flex 93A*, *Ninjaflex (85A)* – which was the material used in the first study – and *Filaflex 70A*. Despite *Smartfil* having a higher shore hardness value than *Ninjaflex*, the corresponding finger was printed using a different 3D printer, the *Ultimaker 3* as opposed to the *Prusa i3 MK3S+*, which could be a noteworthy factor influencing the results.

Subsequently, upon selecting the most suitable material, two different joint geometries were also subjected to testing. As illustrated in Figure 3.4, one of the sample fingers remained the original design, while the other was identical but featured a triangular groove in the joint areas to facilitate the finger’s bending capability.

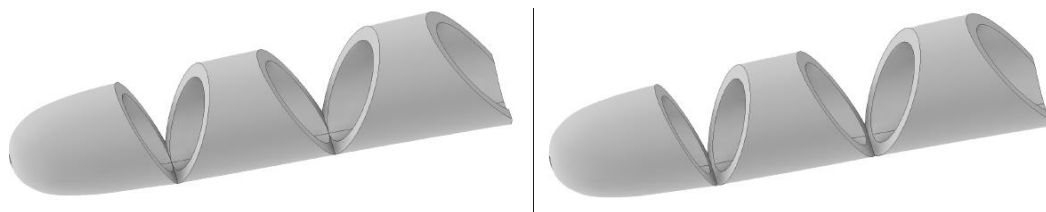


Figure 3.4. Original joint geometry (left) and new joint geometry/crease (right).

These two tests enable not only the examination of variations within the same joint geometry across different materials but also within the same material across different joint geometries.

Furthermore, an additional series of tests involves manipulating finger's wall thickness within the optimal material and joint geometry. Once more, one of the sample fingers retained the original thickness, while the other finger had its thickness reduced by a fourth of its original value, from 2 mm to 1.5 mm. The initial intention was to incorporate a third sample finger with half of the original thickness. However, it turned out to be too thin for the printer, making the sample infeasible for testing.

Regarding the mechanism assembled for these tests, an Arduino code was created to control the servo motor's movement and to collect the load values.

3.3. Fabrication Process of the Actuators

Regarding the actuator's manufacturing process of the hand that served as inspiration for this dissertation, it proves both time-consuming and intricate.

The fabrication of the actuators involves four fundamental steps, as seen in Figure 3.5.

The initial step (I) involves designing the moulds using a CAD Software, particularly *Autodesk Inventor 2023*, and then 3D printing them using the *Prusa i3 MK3S+* printer, with a generic PLA filament.

The second step (II) consists in fabricating the initial/outer silicone layer of the actuator (containing two silicone layers) and its reinforcement. The intricacy originates in part from the initial phase of the second step, which involves winding a polyester reinforcement thread around the core of the mould. This thread ensures that the actuator can only stretch longitudinally and not radially. To execute this step accurately, the entire core of the mould must be covered with the thread to prevent bubble formation upon inflation in thread-free areas (caused by an uneven thread distribution), which could potentially lead to bursting and subsequent leaks. Additionally, due to the actuator's shape, covering the tip of the core with a thread becomes impractical, resulting in its susceptibility to punctures.

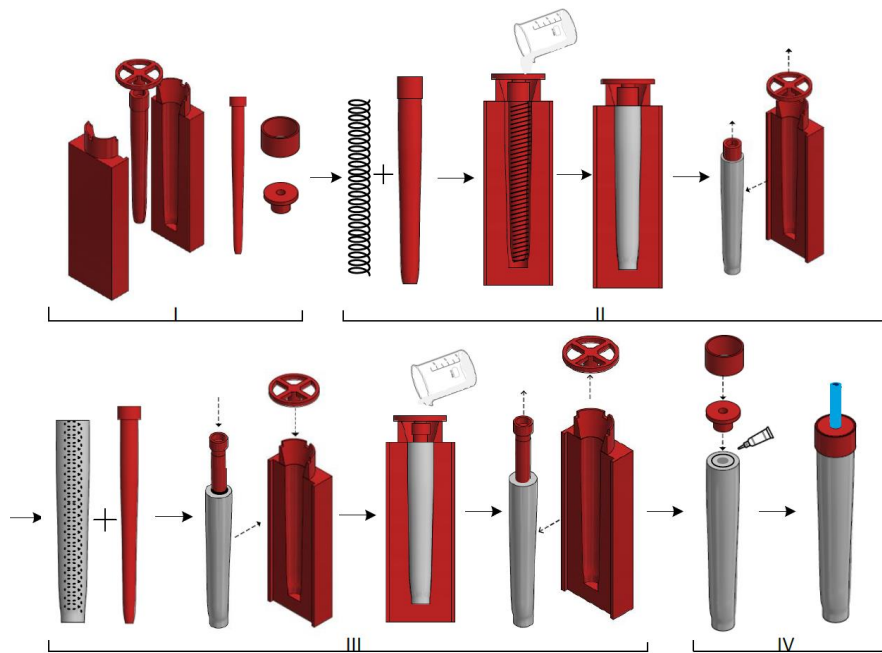


Figure 3.5. The four steps used in the construction of the actuators for the first version of the hand [1].

Moreover, complexity arises during the final phase of this second step. While detaching the core from the rest of the mould, the thread is prone to shifting in the absence of the second/inner layer that stabilizes it. Removing the core of the mould demands a meticulous approach given that if the thread shifts, it invites the formation of new air bubbles, subsequently resulting in additional leaks.

The time-consuming nature of the original fabrication process arises not only from its four fundamental steps, each one long in duration, but also from the silicone's curing time, which is approximately three hours. Furthermore, the meticulous task of winding the thread around the core of the mould adds to the time requirement. This step needs precision and careful attention, justifying a slow and deliberate approach.

To confront these challenges, an alternative and optimized reinforcement method, briefly described in Section 3.1, has been explored. In this method, the reinforcement consists of a unidirectional elastic fixation bandage instead of a PET thread. This reinforcement ensures that, upon inflation, the actuator will also stretch along the axial direction as intended, only with superior results by eliminating the risk of bubble formations, as the core of the mould is now completely covered, consequently reducing the risk for leaks. Moreover, this method enables the bandage to cover the core's tip and simplifies the core's removal process as well as it ensures a more even distribution of the reinforcement.

In terms of the manufacturing process, the first step (I; illustrated in Figure 3.5) consists in designing the moulds, composed of two mould parts and two cores (with one of the cores being larger than the other), and the sealing pieces, that will be used later in the fabrication of the actuator. Following this, all the parts will be printed in the *Prusa i3 MK3S+* 3D printer with a PLA filament.

The second (II) step involves the arrangement of the reinforcement around the largest core. In Figure 3.5, the displayed reinforcement is the polyester thread, as this image was obtained from the initial study conducted on this soft robotic hand. For this study, this step was modified and instead of a PET thread being revolved around the core of the mould, a unidirectional elastic bandage was wrapped around the core and fixed with *Pattex* contact adhesive, as depicted in Figure 3.6.



Figure 3.6. Unidirectional elastic bandage revolved around the core of the mould.

After the assembly of the reinforcement is completed, the silicone preparation process begins. Part A and Part B of the silicone (two distinct liquid components that, upon mixing, undergo curing) are mixed together, at a 1:1 ratio, for approximately three minutes, as recommended. During this process, some bubbles may form in the mixture due to the high viscosity of the mixture. This tendency for the existence of trapped air in the mixture was one of the reasons why the initial version of the actuators was more susceptible to punctures and leaks. However, it's important to note that initially, the laboratory did not have a vacuum chamber available. Now, with the addition of the *VC3028A* vacuum chamber paired with the *VP160* vacuum pump, the result is a uniform silicone mixture free of any bubbles.

After preparing the silicone mixture, it is carefully poured into the mould. To prevent air from getting trapped inside the mould, it is recommended to pour the silicone while tilting the mould, allowing any air to escape. After pouring the silicone, the mould's core is positioned. Once the silicone has completely cured, which typically takes three to four hours,

depending on the type of silicone used, the mould is opened, and the core is extracted from the centre of the first silicone layer. This core removal process does not require a high level of precision, since there is no risk of the reinforcement shifting from its intended position with this new reinforcement method.

In the third (III) step, part of the second step is repeated. Another batch of silicone mixture is prepared and poured, and the core is once again positioned inside the mould parts. However, in this step, the already cured first layer of silicone is placed inside the mould and the silicone mixture is poured into the air chamber of the outer silicone layer, forming the inner layer. Once the silicone is completely cured, the mould is opened, and the core is removed as before.

The sealing of the actuator's base (step IV), in the hand that served as inspiration for this dissertation, operates by using a fitted piece inserted into the actuator's internal channel at its base and a ring that goes around this piece in the outer side of the actuator. This is not an optimal solution as the pieces are not efficiently fixed to the silicone, causing the system to be prone to air leaks and dislodging. Besides, even though the pieces are adhered to one another using super glue, it can weaken and break under excessive pressures.

To address this concern, an alternative method has been developed. As such, in the final step (IV), the sealing piece is inserted into the air chamber of the actuator, and a thread is encircled around it from the exterior of the actuator, to enhance sealing and secure the piece. However, to ensure the effectiveness of this method, the current piece lacks the necessary groove to firmly secure and immobilize the thread. This is crucial in preventing the thread from shifting due to air pressure, which can lead to leaks and compromise the integrity of the seal. For that reason, that sealing piece was also modified and the groove was included (Figure 3.7).

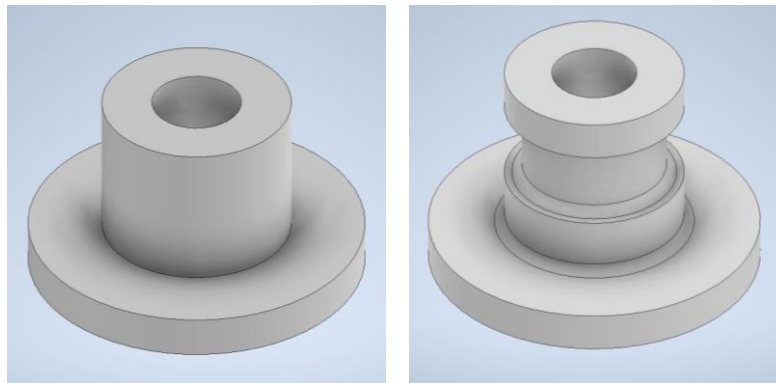


Figure 3.7. Before (left) and after (right) the modifications made to the sealing component for the actuator's base.

In addition, equally to the initial version of the actuators, another ring-like component is placed around the first one to ensure a snug fit on the exoskeleton and further improve the sealing.

Finally, the air inlet tube is inserted through the hole of the sealing piece and sealed with *Araldite CRYSTAL* two-component epoxy at the actuator's base, around the tube.

During the study of the hand that served as inspiration for this dissertation, the actuators underwent testing to determine the maximum horizontal displacement of the actuator under different pressures. This test was replicated in this dissertation with the new actuators with the aim of evaluating whether this new reinforcement method was more efficient than the PET thread reinforcement one.

As the finger was pressurized, a *Honeywell* pressure sensor – model *ABPDANV060PGAA5* – programmed in *Arduino* registered the pressure values simultaneously. The test included five pressure levels ranging from 20 to 60 kPa, with increments of 10 kPa. Two different actuators were tested, one with the same silicone as the initial version of the robotic hand, *Ecoflex 00-50*, and the other with *Ecoflex 00-30*, both fabricated using the unidirectional elastic bandage. This served to identify the silicone that results in the best actuator (and, therefore, finger) performance. The results will be compared and discussed in the next chapter.

Even though the elongation at break is higher with *Ecoflex 00-50*, as listed in Table 3.1, it does not necessarily mean that, when the same pressure is applied to geometrically identical samples of both materials, the one fabricated in *Ecoflex 00-50* would exhibit greater elongation than the one made with *Ecoflex 00-30*. In fact, due to *Ecoflex 00-50*'s higher tensile strength, it can withstand higher load values before breaking. This means that the

higher elongation value could also be attributed to a greater pressure applied to the material. Another supporting factor is the 100% modulus value, which is higher in *Ecoflex 00-50*. This indicates that *Ecoflex 00-50* requires a higher force to stretch it to twice its original dimensions. Another aspect to consider is the difference in shore hardness between *Ecoflex 00-30* and *Ecoflex 00-50*. Given that a lower shore hardness is indicative of a softer and more flexible material, the silicone that promised more stretchability was *Ecoflex 00-30*, which has a lower shore hardness value and, for that reason, is the recommended choice.

When the actuators were reinforced with a PET thread, they exhibited a higher susceptibility to tearing and leaks, as explained earlier. In such cases, the use of *Ecoflex 00-50* was justifiable due to its higher tensile strength, which could prevent these issues. However, with fewer instances of tearing and leaks in the new reinforcement method (only one actuator ripped during the entire project, attributed to incorrect fabrication), using *Ecoflex 00-50* becomes less advantageous. Nonetheless, it should also be tested.

Table 3.1. Technical overview of two silicone types.

Silicone Types	Cure Time (hours)	Pot Life (min.)	Shore Hardness	Elongation at Break (%)	Tensile Strength (MPa)
Ecoflex 00-30	4	45	00-30	900	1.37
Ecoflex 00-50	3	18	00-50	980	2.17

Likewise, the fingers underwent testing to determine the maximum finger force. This test was conducted using a weighing scale (*TechMaster ES-3000A*). The hand was positioned horizontally, with a distance of 40 mm between the palm of the hand and the scale, and the index finger would then be pressurized. As the fingertip touched the scale, the machine would register a mass value. The approximate value of the fingertip's force in Newtons could be obtained by multiplying the mass value by the acceleration of gravity.

For this particular test, seven pressure values (along with their corresponding force values) were considered, specifically ranging from 20 to 80 kPa, in increments of 10 kPa.

In order to determine if the new actuators exert more force than the initial ones, the force-pressure test was replicated using the new actuators. In that regard, these new actuators appear to exhibit greater strength compared to the ones made with polyester thread, as described in the next chapter, where results are discussed.

When combined with the adjustments to the exoskeleton, these changes collectively facilitate finger bending, expanding the range of motion and preventing actuator protrusion from the exoskeleton.

Finally, to evaluate whether the new actuators improve finger flexibility, an additional test was conducted. In this test, the folding angles were measured in correlation with the pressure applied to the actuators. The test included five pressure levels ranging from 20 to 60 kPa, with increments of 10 kPa. The angle values will be compared, in the next chapter, to the values obtained in the initial hand version, as this test was also replicated from that study.

3.4. Enhancing Hand Grip

Another aspect noticed is that the gripping of objects was not entirely efficient. This inefficiency can be attributed not only to the hand's excessively flat geometry, lacking the natural curves of a human hand in its grasping position, but also to the deficiency in the coefficient of friction of the material used in the exoskeleton. Consequently, objects had a tendency to slip during handling, limiting the capability to grasp only very lightweighted objects with very specific shapes.

Additionally, the orientation of the thumb on the exoskeleton was inaccurately configured, resulting in closure towards the index finger rather than the intended closure towards the palm.

3.4.1. Exoskeleton's Geometry

To address this problem, an adjustment was made to the thumb's orientation. To prevent it from closing in the direction of the index finger, it was rotated to close towards the palm. Additionally, the palm near the base of the thumb was bent (Figure 3.8) to enhance gripping and to give the hand a more anatomical appearance.

However, further testing revealed that more modifications were needed. Despite the initial adjustment, the thumb was closing almost parallel to the palm, pushing the objects out of the hand. Additionally, it was observed that the thumb actuator could only bend the joint farther from the base of the finger, as the actuator was positioned too high in the exoskeleton. Consequently, the thumb was not bending at the lower joint as desired.

To address these issues, the thumb was repositioned to ensure it closed in the direction of the palm rather than merely parallel to it. The hole where the base of the thumb's actuator fits into the exoskeleton was also lowered. Additionally, a thin and flat element was added beneath the thumb, similar to those in the other fingers (Figure 3.8). This design alteration facilitates bending at the base of the thumb by reducing material thickness and eliminating curvatures that obstruct the bending movement.

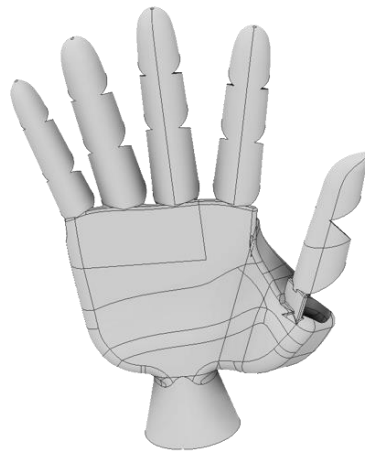


Figure 3.8. Some modifications made to the exoskeleton.

3.4.2. Improving Coefficient of Friction

To improve object grasping, an option was to improve the coefficient of friction. This enhancement was achieved by the integration of silicone strips onto the palm of the hand, as visually represented in Figure 3.9 (a). This inclusion effectively prevented objects from slipping out of the hand, addressing a common issue and thereby increasing the efficacy of this robotic gripper (Figure 3.9 (b)).

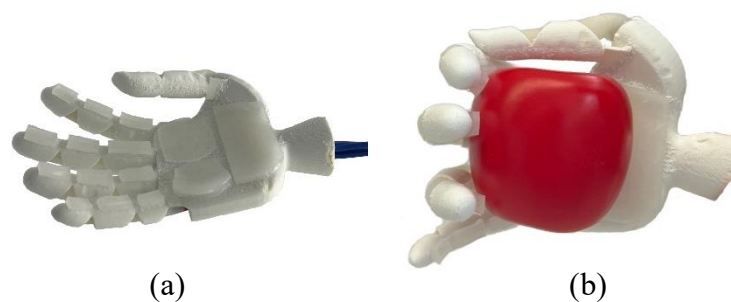


Figure 3.9. (a) Incorporation of silicone strips into the palm of the robotic hand; (b) Successful gripping and retention of objects by the robotic hand, showcasing the practical benefits of the silicone strip integration

4. EXPERIMENTS AND RESULTS

4.1. Fatigue/Cyclical Tests

4.1.1. Materials

As expected, the sample finger printed with *Filaflex 70A* showed less resistance to bending compared to the other two, as illustrated in Figure 4.1 (a). This can be attributed to its lower shore hardness value, listed in Table 4.1, typically associated with greater flexibility and softness. Moreover, the higher elongation at break value of this material (*Smartfil* did not specify its elongation at break value), could also contribute to this outcome.

Table 4.1 Technical overview of three TPU materials.

Filament materials	Elongation at break (%)	Shore hardness
Filaflex 70A	900	70A
Ninjabflex	660	85A
Smartfil Flex 93A	-	93A

On average, the *Ninjabflex* sample needs almost twice as much force to be bent to the same angle as the *Filaflex* one needs. Like so, the *Smartfil Flex 93A* needs, on average, three and a half times more force than the *Filaflex* and almost 2 times more than the *Ninjabflex*.

The Figure 4.1 (c) and (d) show a declining trend in the graph lines, indicating that the force applied to the sample fingers during the initial cycles was greater compared to the later ones. It's important to mention that the graph lines displayed are trendlines, while the actual experimental results exhibited less consistency. If the control system is based on the pressure applied to the actuators, this declining behaviour may not be beneficial, as it can lead to observable changes in the hand's behaviour that deviate from the initial intent.

The *Filaflex* sample exhibits the least occurrence of this behaviour and displays a smaller variation in force values. Due to this factor and its lower bending resistance, *Filaflex 70A* emerges as the superior choice among the three materials.

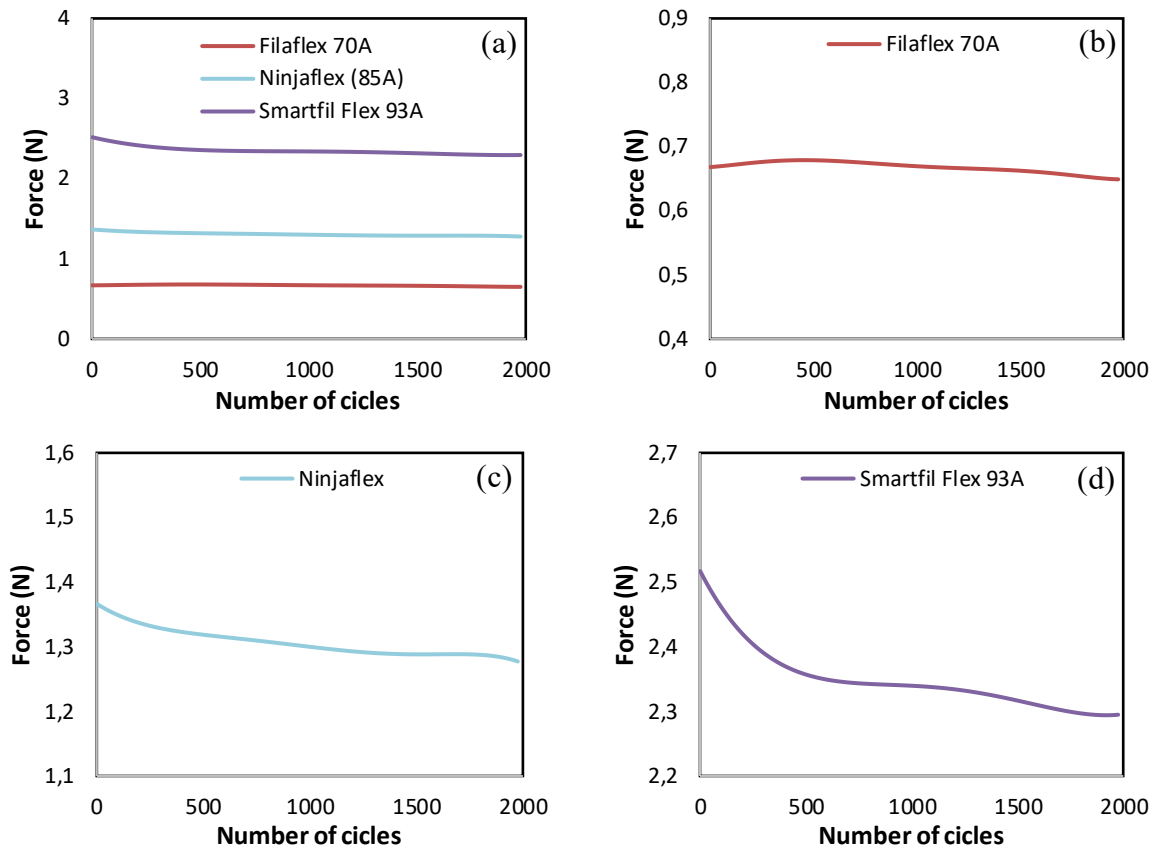


Figure 4.1. (a) Compilation of the results for maximum force applied (per cycle) to each sample finger printed in (b) Filaflex 70A, (c) Ninjaflex and (d) Smartfil Flex 93A.

Regarding the angle at which the load cell touches the samples, which corresponds to the position to which the finger returns at the end of each cycle, the graph line behaviour presented in Figure 4.2 is consistent across all three materials, with the angle values decreasing in the initial cycles and stabilizing after.

This decrease in angle and force happens because the sample finger experiences a slight degradation in structural integrity due to fatigue. As the test progresses, the finger gradually loses some of its elastic memory, making it difficult to return to its original position.

Another noteworthy observation is that the angle values for *Filaflex 70A* appear to be lower compared to the other two materials. This phenomenon may be attributed to the increased flexibility of this material, which could cause it to droop when subjected to perpendicular gravitational forces. This hypothesis is supported by the force graphs, where this sample offered less resistance to bending.

While this behaviour is not ideal, it's worth noting that when the actuators are positioned inside the fingers, this issue would be minimized. Therefore, this material remains the most suitable choice.

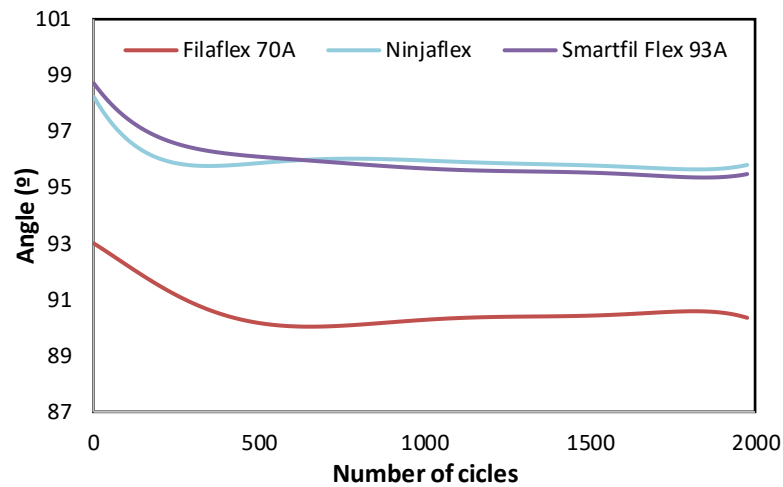


Figure 4.2. Angle (per cycle) at which the load cell touches each sample finger, all printed in different materials.

4.1.2. Geometry

Regarding the geometry of the sample finger, particularly the configuration of its joint, the finger with triangular grooves appears to exhibit even less resistance to bending when compared to the sample with the same material but without any grooves in the joint, as illustrated in Figure 4.3. More precisely, the force required to bend the finger lacking a groove is almost five times higher than that needed for the finger with a groove.

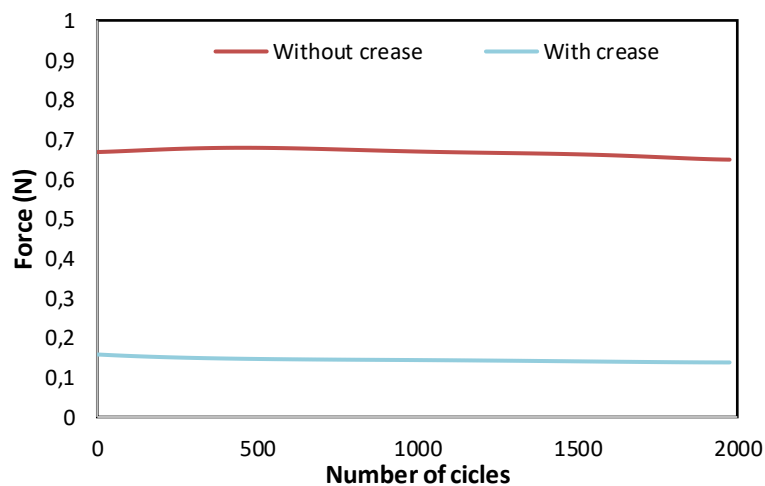


Figure 4.3. Maximum force applied (per cycle) to sample fingers with and without a triangular groove in the joint areas.

In terms of the graph lines' behaviour, both exhibit similar patterns, largely maintaining a horizontal form throughout the line, indicating that the force applied to the sample fingers experiences minimal to no fluctuations.

While this configuration can offer advantages, its success relies on the finger preserving its elastic memory, i.e., it should return to its original position or at least exhibit similar behaviour as the unincreased finger. This could be confirmed by examining the angle values at which the load cell touches the sample fingers. However, these results were inconclusive. In fifteen different tests conducted, the outcomes did not converge to a consistent behaviour, nor did they demonstrate the expected behaviour. This is noted because most of the graph lines exhibit erratic behaviour, as the angle values increase with each cycle instead of decreasing, and some even fluctuate (refer to Figure 4.4). This discrepancy may be attributed to software malfunctions, although the most plausible cause is that the sample fingers shifted from their intended position during the tests, causing the load cell to touch a higher finger segment.

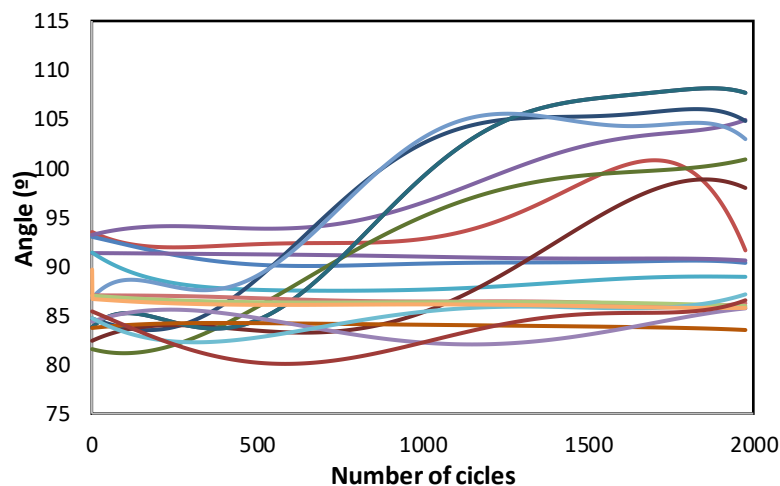


Figure 4.4. Compilation of all the results for the angles (per cycle) at which the load cell touches the sample finger with a triangular groove.

Usually, only about five tests were conducted for each sample finger. Yet, upon analysing the results, it became necessary to print more samples and conduct additional tests, resulting in a total of fifteen tests for this joint geometry. Unfortunately, this did not resolve the problem, and therefore these results cannot be considered for this study.

Had the results been favourable, and considering the force test results were superior to the other sample with a different joint geometry, this configuration might have been chosen for the fingers. However, due to concerns about potential wear and tear on the joints, which

could lead to thinning or even breakage over time, the safer choice was to opt for the finger without a groove.

4.1.3. Thickness

The graph portrayed in Figure 4.5 (a) illustrates that the thinner sample, measuring 1.5 mm in thickness, requires half of the force for bending when compared to the original thickness of 2 mm. This behaviour was predictable, as thickness significantly influences an object's flexibility.

Additionally, despite the test conducted on the thinner sample showing slightly lower angles values (Figure 4.5 (b)), which was also expected due to the increased flexibility (also mentioned in Section 4.1.1), these values exhibit great stability, displaying an almost perfectly horizontal line. This means that the finger retains most of its structural integrity and returns to its original position.

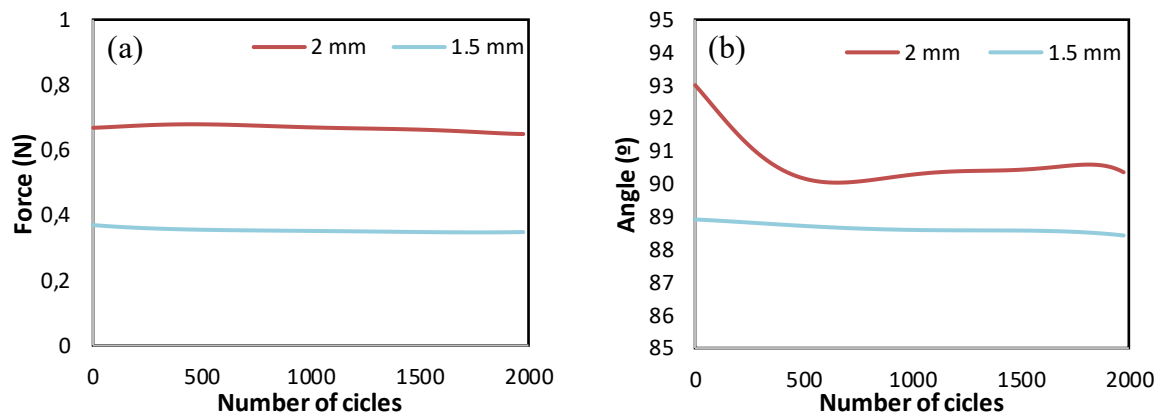


Figure 4.5. Maximum force applied to sample fingers with different thicknesses and angles at which the load cell touches the finger.

Considering both of these factors, this thickness proves to be the superior choice. Therefore, the ultimate selection consists of an exoskeleton printed in *Filaflex 70A*, featuring a finger design with no grooves in the joint areas and a thinner wall thickness.

4.2. Pressure Related Tests

The new reinforcement method for the actuators, using a unidirectional elastic bandage, was also subjected to testing with two different silicone materials. Accordingly, the tests were conducted for horizontal displacements, folding angles and fingertip forces

for each actuator. These results were then compared to those obtained in the initial version of the hand [1].

4.2.1. Horizontal Displacement

Regarding the horizontal displacement, a direct comparison between the initial version of the actuator and the new one, using the same silicone material (*Ecoflex 00-50*), shows minimal variations in results, as observed in Figure 4.6 and Figure 4.9. This means that the new reinforcement method does not improve horizontal displacement unless additional changes are incorporated besides the reinforcement.

As depicted in Figure 4.6 and in the graph displayed in Figure 4.9, the initial displacement values are nearly identical, but the values obtained with the new actuators were slightly lower. At 50 kPa, the new actuator's displacement exceeds that of the original actuator, only to be surpassed again at 60kPa. It is also worth noting that the displacement in the new actuator appears to stabilize between 50 kPa and 60kPa.

The same test was conducted on another actuator, which was also fabricated using the new reinforcement method, using *Ecoflex 00-30* instead of *Ecoflex 00-50*. This time, the displacement values obtained were higher than those of the initial hand version, as illustrated in Figure 4.7 and Figure 4.9.

Additionally, these values seem to stabilize, once again, between 50 kPa and 60 kPa. However, this actuator also tends to curve when pressurized and, for that reason, the displacement values may not be entirely accurate and should, in fact, be slightly higher. To obtain more precise results, *FreeCAD* was used, giving the data presented in Figure 4.8.

The curvature can be attributed to either the contact glue used to secure the unidirectional elastic fabric or the possibility that the core of the mould was slightly misaligned, resulting in one side of the actuator's walls being thicker than the other.

Although not ideal, this curvature can be somewhat advantageous if the actuator is correctly positioned inside the finger, aligning with the finger's intended bending direction.

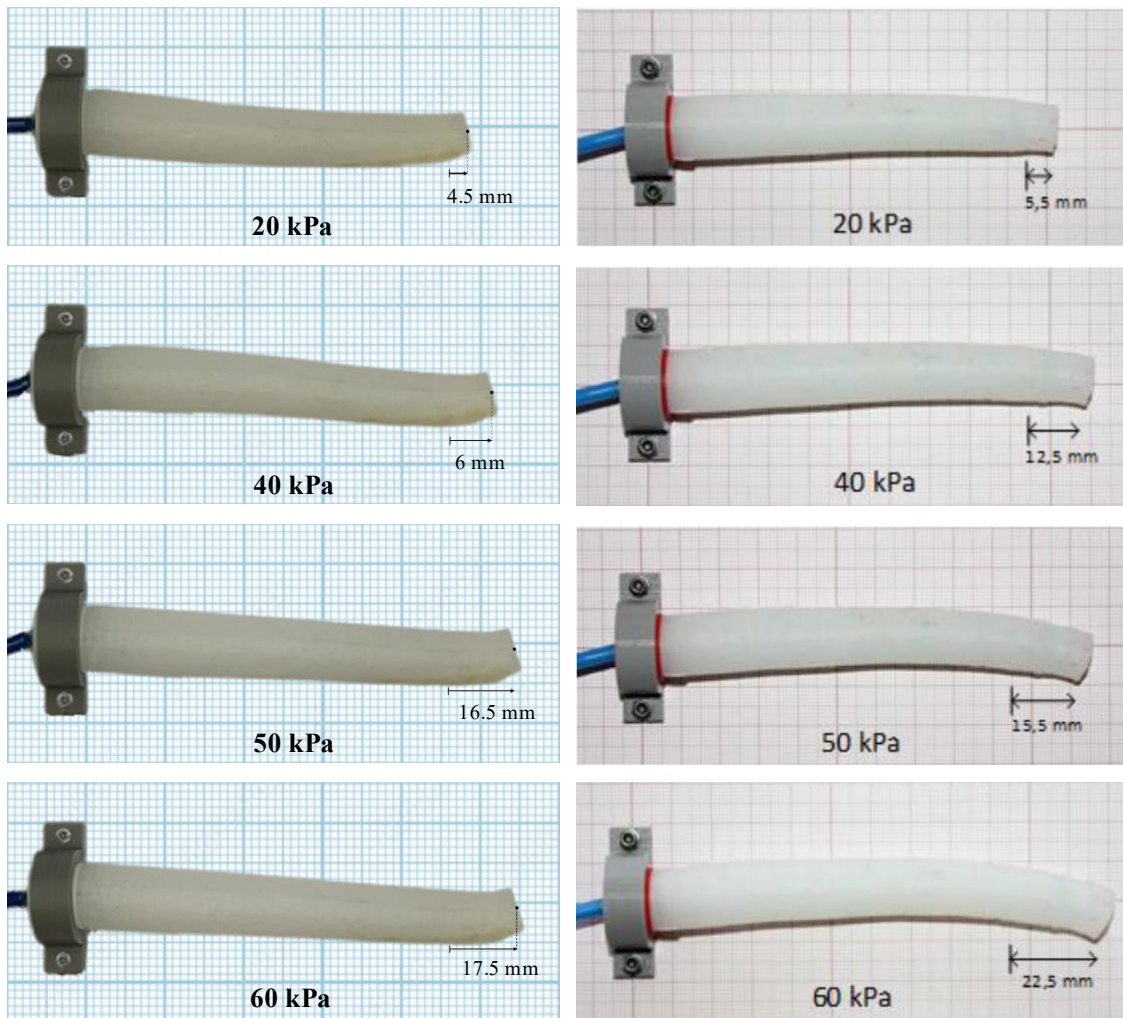


Figure 4.6. Horizontal displacement results compared between the new reinforcement method (on the left) and the initial one (on the right) [1], both fabricated with *Ecoflex 00-50*.

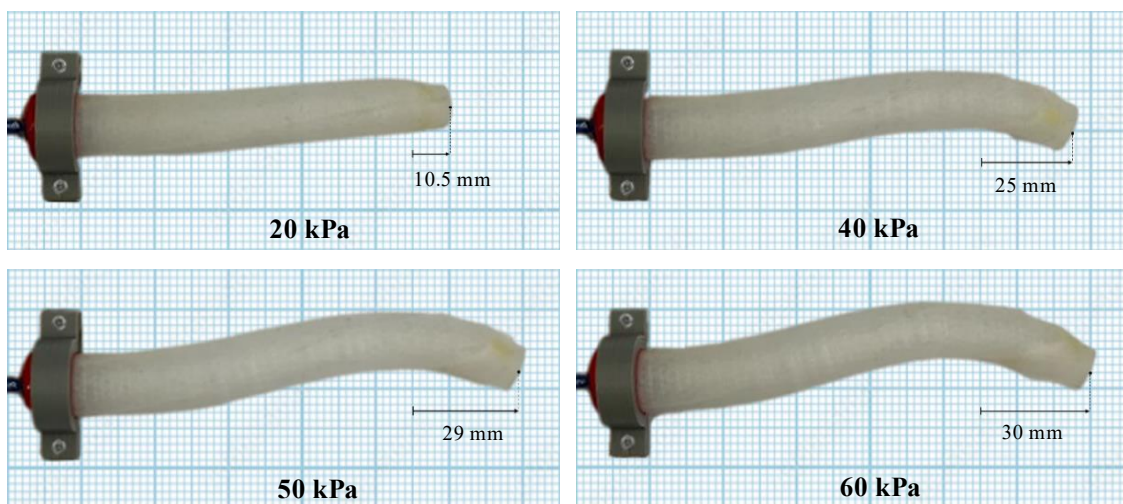


Figure 4.7. Horizontal displacement results for the actuator fabricated with the new reinforcement method using *Ecoflex 00-30*.

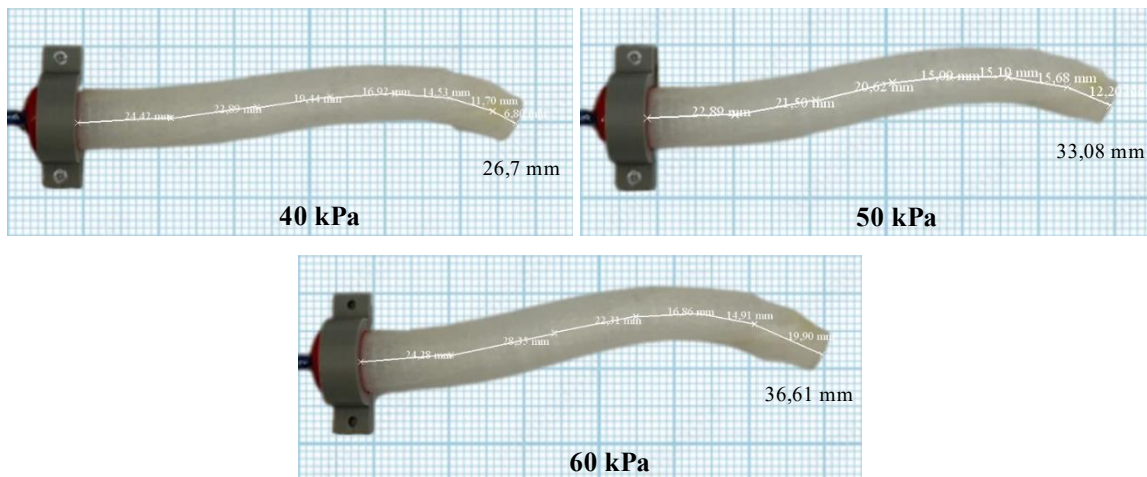


Figure 4.8. True displacement values corrected for the actuator curvature.

Subsequently, all these displacement values, along with those registered in the initial version of the hand, were compiled into the graph represented in Figure 4.9. In this graph, it's evident that the actual displacement values of the newly fabricated actuator using *Ecoflex 00-30* are more linear in relation to the values registered for lower pressures than the horizontal displacement values registered without considering the curvature.

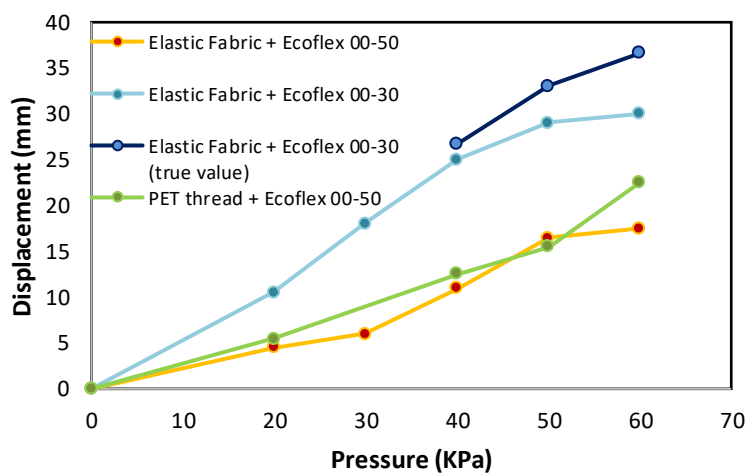


Figure 4.9. Horizontal displacement in relation to the pressure applied to the actuator for different silicones, *Ecoflex 00-50* and *Ecoflex 00-30* (accounting for curvature correction), and reinforcements, PET thread and unidirectional elastic fabric for reinforcements.

4.2.2. Folding Angle

In regard to the folding angle, i.e., the angle formed by the fingertip in relation to the surface of the palm, the values registered for the new actuators in combination with the new exoskeleton exceeded those of the initial version of the hand (see Figure 4.10 and Figure 4.11).

It is also noteworthy that the angle value when the actuators are not pressurized is higher for the new fingers, likely due to *Filaflex*'s greater flexibility compared to *Ninjaflex*, the material used for the exoskeleton in the initial hand version. This fact may also contribute to higher angle values during pressurization, as the exoskeleton printed in *Filaflex* shows less resistance to bending, as concluded in Section 4.1.1.

Another contributing factor to these results could be the finger's reduced wall thickness in the new exoskeleton compared to the original one, enhancing the finger's flexibility, thereby reducing its resistance to bending.

Additionally, the new robotic hand demonstrates increased linearity in the angle values, providing better predictability in the finger's motion.

Lastly, when comparing the performance of the new actuators using the same exoskeleton, once again, the one fabricated with *Ecoflex 00-30* exhibited superior results, with higher values for the same applied pressures, which was expected considering the results for horizontal displacement were also higher for this actuator.

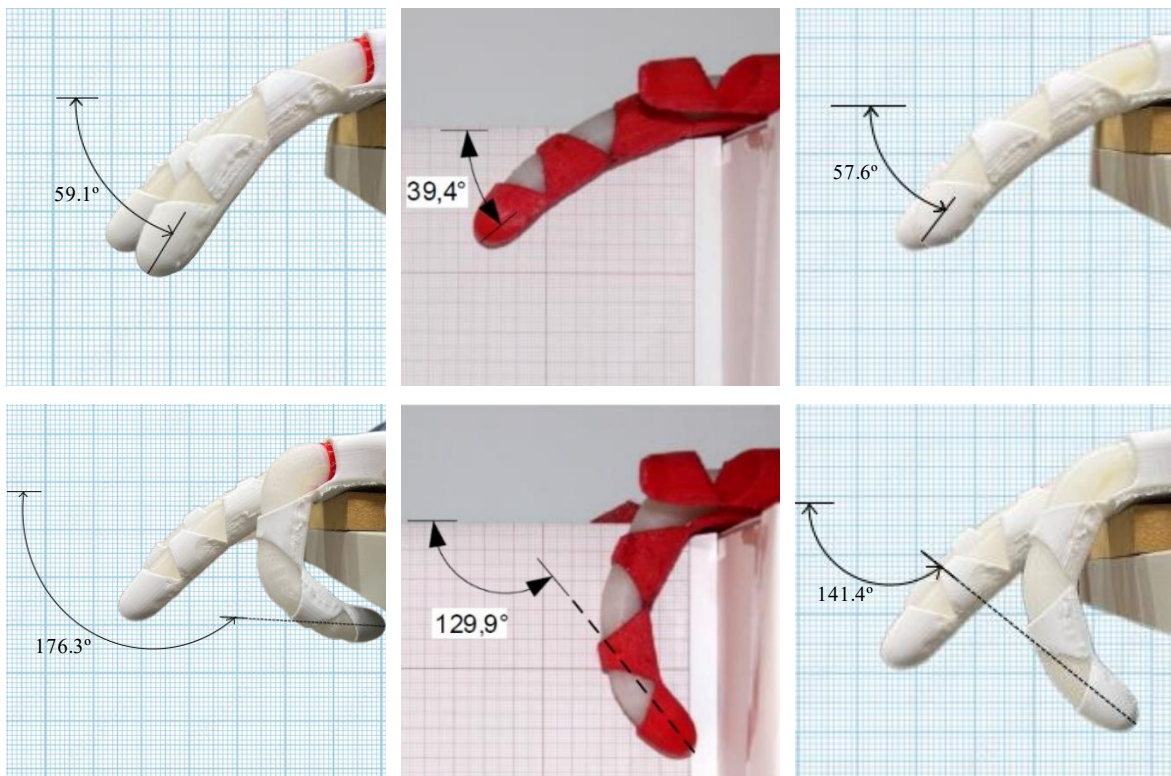


Figure 4.10. Results of the folding angles at 0 kPa (at the top) and at 60 kPa (at the bottom) using the new actuators with unidirectional elastic fabric reinforcement, one with *Ecoflex 00-30* (at the left) and the other with *Ecoflex 00-50* (at the right), and the initial version of the actuator (in the centre) [1].

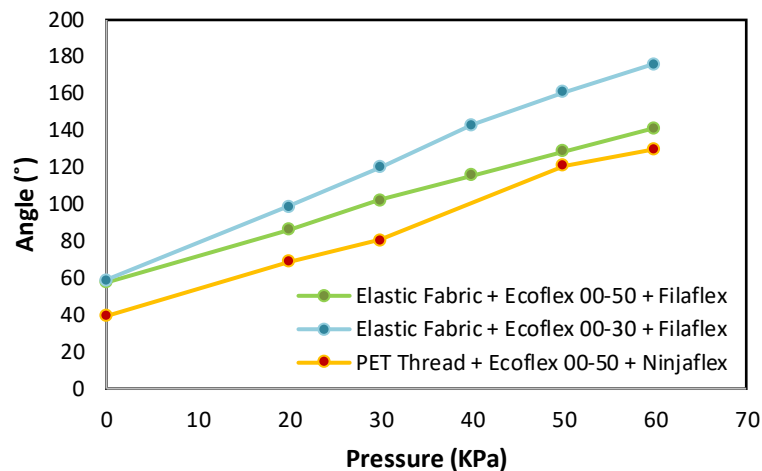


Figure 4.11. Folding angles in relation to the pressure being applied (from 0 kPa to 60 kPa).

4.2.3. Finger Force

The last pressure related test was to determine the finger's force using each of the two new actuators and comparing their results to the results obtained in the study of the hand's first version. This time, the maximum pressure applied to the actuators was 80 kPa.

The maximum force value obtained experimentally in the initial hand version, using polyester-reinforced actuators and *Ninjaflex* as the material for the exoskeleton, was 0,81 N at the maximum pressure of 80 kPa [1].

Once more, the results appear to be on average better for the new actuators, with higher values for the one made with Ecoflex 00-30.

The increased force applied in the scale by the new robotic hand could be attributed to the same factors that result in higher bending values when pressurized. These factors include the higher flexibility of *Filaflex* compared to *Ninjaflex* and the reduced wall thickness of the new exoskeleton's finger. Both of these elements contribute to increased finger flexibility and, therefore, reducing its resistance to bending. As a result, when the finger resists less, the force applied by the actuators is more efficiently used, and not lost due to the resistant force.

Another contributing factor may be the reinforcement method. With the new method, all the pressure is efficiently used to stretch the actuator longitudinally. In contrast, when the actuator made with PET thread reinforcement is pressurized, it experiences some pressure loss due to minor radial deformations. This can occur because the thread might not be correctly positioned, as described in the previous chapter, and also in the areas with no thread

when the actuator is pressurized. Even if the thread is well positioned during fabrication, when the actuator is pressurized, the helical thread separates from itself, leaving some unreinforced areas, although in this case the pressure that is lost is not significant.

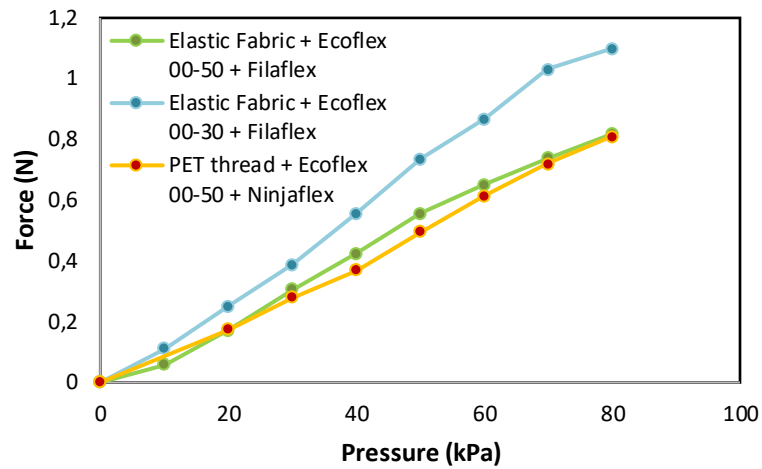


Figure 4.12. Finger force applied to the weighting scale in relation to the pressure (from 0 kPa to 80 kPa).

5. CONCLUSIONS

In order to assess the impact of certain modifications on enhancing the exoskeleton, sample fingers were subjected to cyclic loading testing. The purpose of this test was to quantify both the resistive force produced by the fingers when bent to a specific angle, and the angle to which the sample fingers returned in the absence of an applied load. Within each operational cycle, the servo motor executed a controlled rotation spanning from predefined angles. This motion engaged the load cell, which was mechanically linked to the motor, inducing a bending action in a sample finger.

Evaluating the results, *Filaflex 70A* emerged as the material with the least resistance to bending compared to the other two options, *Ninjaflex* and *Smartfil Flex 93A*. Consequently, it was the material chosen for printing the exoskeleton. This behaviour can be attributed to *Filaflex*'s lower shore hardness and higher elongation at break values. Furthermore, this material displays a smaller variation in force values compared to the other materials.

The decision to retain the original finger joint geometry was not due to unfavourable results of the grooved joint design but rather because some of the findings for this last geometry were inconclusive, making it unwise to take unnecessary risks such as tearing of the fingers by fatigue. Nonetheless, it is worthy to note that the sample finger featuring grooves in the joints showed less resistance to bending compared to all the other samples.

As for the finger's wall thickness, the thinner sample finger delivered the best performance, leading to the selection of this wall thickness. The thinner finger exhibited reduced bending resistance compared to the original thickness, as anticipated, given that an object's flexibility is greatly influenced by its thickness. Moreover, the thinner finger also demonstrates superior retention of its elastic memory, as evidenced by the remarkable stability in the angle values at which the load cell touches the finger during each cycle.

Regarding the actuators, the horizontal displacement was notably higher for the actuator fabricated with the unidirectional elastic bandage in combination with *Ecoflex 00-30*. As a result, *Ecoflex 00-30* was the preferred silicone type for the actuators. In contrast, the results obtained with the actuator fabricated using the same method but with a different silicone type, *Ecoflex 00-50*, showed lower values that closely resembled those obtained with

the actuator manufactured using a PET thread reinforcement and the same silicone type. This suggests that the new reinforcement method, which uses a unidirectional elastic bandage, does not significantly influence the displacement values, but the choice of silicone type does.

The actuator that demonstrated superior performance in the horizontal displacement test also outperformed the other two actuators in the bending angle and finger force tests. When comparing the other two actuators, both using the same type of silicone, the one crafted with the new reinforcement method displayed slightly higher values for both of these tests, although very similar to the other actuator. Given that the horizontal displacement values for both these actuators was also very close, and even slightly lower for the new reinforcement method, it can be deduced that the modifications made to the exoskeleton are the primary contributing factor for these results. However, it's worth noting that although the new reinforcement method possibly did not directly enhance actuator displacement, bending angle and finger force, it indirectly contributed to it. In situations where the actuators were reinforced with a PET thread, they displayed a heightened vulnerability to tearing and leaks. In these instances, using *Ecoflex 00-50* was a reasonable choice due to its superior tensile strength, which had the potential to mitigate these concerns. Since the new reinforcement method effectively eliminates this concern, there is no longer a need to rely on *Ecoflex 00-50*. Instead, using *Ecoflex 00-30* will significantly improve actuator performance.

The actuators made using the new reinforcement method that employs a unidirectional elastic bandage, have proven to be more reliable than their PET thread equivalents. They are less prone to tearing and leaks, enhancing overall efficiency. It is also noteworthy that the actuators are constrained not only by the silicone's elasticity but also by the fabric's limited stretchability. This differs from the PET reinforced actuators, where flexibility largely depends on the silicon's properties, since the actuator never expands enough for the thread to act as a limiting factor.

The introduction of the vacuum chamber during the actuator fabrication process had a significant influence on the outcomes. This alteration substantially reduced the presence of air bubbles within the uncured silicone, consequently providing a more consistent and robust actuator that exhibits enhanced tear resistance.

Another noteworthy conclusion is that the fabrication of the new actuators, while making them more efficient, requires slightly more time, contrary to what was initially

believed. This additional time is needed not only in wrapping the fabric but also due to the 1-hour longer curing time of *Ecoflex 00-30* compared to *Ecoflex 00-50*. However, given the more extended pot life of *Ecoflex 00-30*, it provides a wider time frame for preparing the mixture and using the vacuum chamber without feeling rushed.

In terms of complexity, the success of this reinforcement method depends on the individual mastering the technique. During the initial attempts at wrapping the elastic fabric around the core of the mould, a significant amount of fabric was wasted due to the inability to finish the task successfully. However, with practice, the last actuators were produced with no waste (in material and timewise), demonstrating the learning curve associated with this method.

5.1. Future Work

The joint featuring a groove was not the geometry selected. Nevertheless, considering the substantial improvement in load-related performance observed with this finger sample, it becomes evident that further exploration and refinement of this concept could be advantageous. Additionally, alternative joint configurations could be explored, such as joints with an extended rectangular shape (similar to the one introduced at the base of the thumb), or with a zig-zag pattern.

Regarding the fabrication of the actuators, it might be beneficial to experiment with different unidirectional elastic bandages. Exploring alternative brands might offer a chance to find a bandage with superior stretchability, thus enhancing the elongation capabilities of the actuators. Furthermore, experimenting with different silicones, like *Ecoflex 00-20 FAST*, could be a viable option. This silicone offers a lower shore hardness (00-20) than *Ecoflex 00-30* and a significantly quicker curing time of just one hour, as opposed to the four hours required by *Ecoflex 00-30*. Additionally, it maintains a decent pot life of 20 minutes, making it a potential candidate for improvement. Although this silicone has a lower tensile strength, this may not significantly impact the actuator's susceptibility to tearing, especially considering that the new reinforcement method reduces the risk of such occurrences.

In conclusion, to enhance object gripping, it's recommended to explore a new thumb orientation, possibly bending from beneath the palm of the hand. This orientation can provide essential support that is currently lacking, given that most of the fingers are

positioned in the upper part of the hand. While this adjustment might compromise some of the hand's biological appearance, it would significantly improve its efficiency and usability.

REFERENCES

- [1] S. Alves, “Design and manufacturing of soft robotics mechanisms: improving the reliability of pneumatic-based solutions.”
- [2] K. Ma, X. Chen, J. Zhang, Z. Xie, J. Wu, and J. Zhang, “Inspired by Physical Intelligence of an Elephant Trunk: Biomimetic Soft Robot with Pre-programmable Localized Stiffness,” *IEEE Robot Autom Lett*, pp. 1–8, Mar. 2023, doi: 10.1109/lra.2023.3256922.
- [3] A. Bhat, J. W. Ambrose, and R. C. H. Yeow, “Composite Soft Pneumatic Actuators Using 3D Printed Skins,” *IEEE Robot Autom Lett*, vol. 8, no. 4, pp. 2086–2093, Apr. 2023, doi: 10.1109/LRA.2023.3246841.
- [4] J. Fraś, M. Maciaś, F. Czubaczyński, P. Salek, and J. Glówka, “Soft flexible gripper design, characterization and application,” in *Advances in Intelligent Systems and Computing*, Springer Verlag, 2017, pp. 368–377. doi: 10.1007/978-3-319-48923-0_40.
- [5] J. Frasn and K. Althoefer, “Soft Biomimetic Prosthetic Hand: Design, Manufacturing and Preliminary Examination,” in *IEEE International Conference on Intelligent Robots and Systems*, Institute of Electrical and Electronics Engineers Inc., Dec. 2018, pp. 6998–7003. doi: 10.1109/IROS.2018.8593666.
- [6] Tian H, Liu H, Shao J, Li S, Li X, and Chen X, “An electrically active gecko-effect soft gripper under a low voltage by mimicking gecko’s adhesive structures and toe muscles,” 2020.
- [7] E. Kizilkan, J. Strueben, A. Staubitz, and S. N. Gorb, “Bioinspired photocontrollable microstructured transport device,” *Sci Robot*, vol. 2, no. 2, 2017, doi: 10.1126/scirobotics.aak9454.
- [8] W. A. Breckwoltd, K. A. Daltorio, L. Heepe, A. D. Horchler, S. N. Gorb, and R. D. Quinn, “Walking inverted on ceilings with wheel-legs and micro-structured adhesives,” in *IEEE International Conference on Intelligent Robots and Systems*, Institute of Electrical and Electronics Engineers Inc., Dec. 2015, pp. 3308–3313. doi: 10.1109/IROS.2015.7353837.
- [9] Q. H. Cheng, B. Chen, H. J. Gao, and Y. W. Zhang, “Sliding-induced non-uniform pretension governs robust and reversible adhesion: A revisit of adhesion mechanisms of geckos,” *J R Soc Interface*, vol. 9, no. 67, pp. 283–291, Feb. 2012, doi: 10.1098/rsif.2011.0254.
- [10] M. T. Northen, C. Greiner, E. Arzt, and K. L. Turner, “A gecko-inspired reversible adhesive,” *Advanced Materials*, vol. 20, no. 20, pp. 3905–3909, Oct. 2008, doi: 10.1002/adma.200801340.
- [11] Rashmi Nanjundaswamy, “Biomimicry: Synthetic Gecko Tape by Nanomolding General Description.”

- [12] H. Shahsavan, S. M. Salili, A. Jákli, and B. Zhao, “Thermally Active Liquid Crystal Network Gripper Mimicking the Self-Peeling of Gecko Toe Pads,” *Advanced Materials*, vol. 29, no. 3, Jan. 2017, doi: 10.1002/adma.201604021.
- [13] D. Tao *et al.*, “Controllable Anisotropic Dry Adhesion in Vacuum: Gecko Inspired Wedged Surface Fabricated with Ultraprecision Diamond Cutting,” *Adv Funct Mater*, vol. 27, no. 22, 2017, doi: 10.1002/adfm.201606576.
- [14] J. Shintake, V. Cacucciolo, D. Floreano, and H. Shea, “Soft Robotic Grippers,” *Advanced Materials*, vol. 30, no. 29. Wiley-VCH Verlag, Jul. 19, 2018. doi: 10.1002/adma.201707035.
- [15] EarthDate, “Hanging with Geckos,” Oct. 2020. Accessed: Apr. 28, 2023. [Online]. Available: https://www.earthdate.org/files/000/002/199/EarthDate_181_C.pdf
- [16] H. Terwisscha-Dekker, M. Grzelka, S. Lépinay, and D. Bonn, “How does ‘Gecko tape’ work?,” *Biotribology*, vol. 26, Jun. 2021, doi: 10.1016/j.biotri.2021.100179.
- [17] T. S. Hu, P. Niewiarowski, and Z. Xia, “Sticky yet Clean-The Secrets of the Gecko’s Adhesive System,” Nov. 2012. [Online]. Available: www.brand.de
- [18] M. H. Rasmussen *et al.*, “Evidence that gecko setae are coated with an ordered nanometre-thin lipid film,” *Biol Lett*, vol. 18, no. 7, 2022, doi: 10.1098/rsbl.2022.0093.
- [19] H. Tian *et al.*, “Gecko-Effect Inspired Soft Gripper with High and Switchable Adhesion for Rough Surfaces,” *Adv Mater Interfaces*, vol. 6, no. 18, 2019, doi: 10.1002/admi.201900875.
- [20] A. G. Gillies, J. Kwak, and R. S. Fearing, “Controllable particle adhesion with a magnetically actuated synthetic gecko adhesive,” *Adv Funct Mater*, vol. 23, no. 26, pp. 3256–3261, Jul. 2013, doi: 10.1002/adfm.201203122.
- [21] D. M. Drotlef, P. Blümner, and A. Del Campo, “Magnetically actuated patterns for bioinspired reversible adhesion (dry and wet),” *Advanced Materials*, vol. 26, no. 5, pp. 775–779, Feb. 2014, doi: 10.1002/adma.201303087.
- [22] J. D. Eisenhaure, T. Xie, S. Varghese, and S. Kim, “Microstructured shape memory polymer surfaces with reversible dry adhesion,” *ACS Appl Mater Interfaces*, vol. 5, no. 16, 2013, doi: 10.1021/am402479f.
- [23] B. K. S. Woods, M. F. Gentry, C. S. Kothera, and N. M. Wereley, “Fatigue life testing of swaged pneumatic artificial muscles as actuators for aerospace applications,” *J Intell Mater Syst Struct*, vol. 23, no. 3, pp. 327–343, Feb. 2012, doi: 10.1177/1045389X11433495.
- [24] Y. Jiang, D. Chen, J. Que, Z. Liu, Z. Wang, and Y. Xu, “Soft robotic glove for hand rehabilitation based on a novel fabrication method,” in *2017 IEEE International Conference on Robotics and Biomimetics, ROBIO 2017*, Institute of Electrical and Electronics Engineers Inc., Jul. 2017, pp. 817–822. doi: 10.1109/ROBIO.2017.8324518.
- [25] C. Wenlin *et al.*, “Experimental study on dynamic characteristics and fatigue of mckibben pneumatic artificial muscles,” in *2021 IEEE International Conference on*

- Real-Time Computing and Robotics, RCAR 2021*, Institute of Electrical and Electronics Engineers Inc., Jul. 2021, pp. 223–226. doi: 10.1109/RCAR52367.2021.9517361.
- [26] A. Zaghoul and G. M. Bone, “Origami-Inspired Soft Pneumatic Actuators: Generalization and Design Optimization,” *Actuators*, vol. 12, no. 2, Feb. 2023, doi: 10.3390/act12020072.
- [27] D. K. Patel *et al.*, “Highly Dynamic Bistable Soft Actuator for Reconfigurable Multimodal Soft Robots,” *Adv Mater Technol*, vol. 8, no. 2, Jan. 2023, doi: 10.1002/admt.202201259.